Assessment of the integration of solar heat power into food drying processes

Author: Charalampos Psilopoulos
Supervisors: Martin Andersson & Luis Guerreiro
Examiner: Marcus Thern

Lund University, LTH
June 2023

Table of Contents

Abstract

The long-lasting usage of fossil fuels has brought its negative impact on the planet and thus the society is turning towards more environmentally sustainable solutions in every aspect of life. This master's thesis discusses the novel topic of integrating concentrated solar thermal collectors, which directly produce steam, to drying processes in the food industry, which is proven to currently emit significant amounts of Greenhouse Gases (GHGs).

The aim is to investigate the possible pathways solar thermal can be integrated to the industry, the minimization of fossil fuels usage, the CO_2 emissions reduction, and the feasibility of the investment in concentrating thermal collectors' fields. To achieve so, many visits have taken place to one of the most distinguished food industries in Greece, and in collaboration with it and the companies Absolicon and MG Sustainable in Sweden, a process layout is proposed that shows a steam mass flow reduction for the same yield, as well as CO_2 emissions reduction and the economical feasibility for the implementation of the solar field.

Acknowledgments

I would like to thank my supervisor from Lund University, Martin Andersson, who has helped me throughout the writing of this thesis and throughout the two years of this master's degree, by always providing useful information. Furthermore, I would like to thank my supervisor outside the University, Luis Guerreiro from the company Absolicon, and Joao Gomes, the founder of MG Sustainable, who have both helped me greatly by having a fruitful collaboration, by providing me information about the solar processes and involving me in the writing of European Horizon calls. Additionally, I would like to thank Christos Stiapis from the Greek food industry in study in this thesis, who has deeply helped me in realizing this thesis by devoting time for me and by constantly providing deep knowledge in engineering topics concerning this project.

Introduction

Climate change and the global temperature rise outcomes are more present than ever, making vital the need to reduce it. In the meantime, energy carriers' acquisition from governments or individuals has played a crucial role in people's life and resulted to various adverse events as well as an increase in the price of almost every good around the world. In the meantime, as the world's population constantly increases with time, so do its needs, there is an increased demand for food production. One of the most widely consumed foods worldwide is milk and its byproducts, which many industries produce. This master's thesis aims to propose an environmentally, economically sustainable, and efficient way in the milk production industry, and in more detail in drying processes, using solar energy to produce steam directly, which subsequently will heat up air that will be sprayed to dry milk for various food compositions. The research questions that led to this thesis and are answered are:

Research question 1: How can solar energy with direct steam generation be implemented in food industries in drying processes?

Research question 2: What is the environmental impact of using solar energy in an industry for spray drying?

Research question 3: Is the investment in solar fields economically feasible?

Research question 4: Are there any complications and bottlenecks in this process and how could they be solved?

1. Worldwide food demand

It is beyond any doubt that throughout the last years, numerous changes have occurred affecting people's way of living. The past few decades the footprint of the Greenhouse gas emissions is more prominent to the planet. Our World in Data mentions that 26% of the GHG emissions produced on the world come from food production, translating to one-fourth of the world's GHG emissions, as well as that emissions from food could take us past 1.5°C or 2°C this century (1). Thus, in order to reduce GHG emissions and get close to the achievement of the 17 Sustainable Development Goals and in more detail SDG 2 and SDG 12, it is crucial to make food production from end to end, more sustainable.

Figure 1: Sustainable goals 2 and 12 (2)

The constantly increasing population has brought an increased food demand. It has been estimated that by 2050 the population of the world may reach 9.7 billion, thus bringing an increase in food consumption by 59% to 98% (3). One of the most consumed foods throughout the world is milk, providing nutrients and protein to people from the commencement of their life. Also, many byproducts of milk are consumed widely, such as yoghurt, ice-cream, dried milk, skimmed milk, and milk powders, which are either used as baby food, additives on foods or deserts, or food supplements. Thus, milk is a highly consumed food throughout the world and is going to further increase. Milk powders deliver excellent nutritional value which can be distributed worldwide due to the reduced volume required and the available long shelf-life. Milk powder production involves many processes and one of the most energy consuming is milk drying. Drum drying is a common way of drying milk and similar liquids, while in the last few years spray drying has been implemented and has achieved remarkable results, offering the ability to dry other foods like fruits. During the visits that took place in the food industry during this thesis, the existing drying system used is drum drying but spray drying is proposed to be deployed to achieve higher efficiency and lower emissions. The further implementation of clean energy sources can significantly reduce the emissions of this process.

1.1 Drum drying

Drum dryers, also known as roller dryers, are constructed in a way that involves one rotating or two counter-rotating drums. The material to be dried, which is usually slurry or viscous in nature, is spread mechanically on the drums as a thin sheet. The sheet is then rapidly dried through conductive means, as high heat is generated within the drum. The type of drum dryer used depends on the moisture level of the material to be dried. For materials with high moisture levels like milk, a temperature of 195°C is achieved within the drum, while for highly heat-

sensitive materials, lower temperature hot air is transferred within the drum. The drum dryer operation is dependent on several factors, including the pressure of steam within the drum, the speed of drum rotation, the width of the applicator, and the ratio of drum speed rotations. These parameters can be controlled independently without any dependence on each other. The typical values of the drum dryer components range from steam pressure in the drum of 2 $x10^6$ Pa to 10 $x10^6$ Pa, rotation speed varying from 2 rpm to 30 rpm, thin sheet applicator width designed from 0.05 mm to 0.5 mm, and the ratio of drum rotation speed ranging from 1 to 5 (4).

In drum drying, the heated surface is a rotating horizontal metal cylinder. The cylinder is heated by steam on the inside, bringing the temperature of the cylinder wall to 120°C –200°C. Drum drying also known as roll drying is a continuous process that creates dry powders and flakes from a liquid feedstock. The liquid feed is sprayed onto one rotating drum. The drum is heated internally with steam to increase the surface temperature. As the material is sprayed-laid over the drum as a thick liquid, it sticks and dries to the surface, while being moved from other smaller guides that are sat on top of the drum. To obtain the desired specifications, the drum's rotation speed, steam pressure, and the gap can be varied. The dried material is peeled from the drums using a knife system. During drum drying, since the food is laid over in a liquid form, it is exposed to the outer environment, increasing substantially the danger of contamination and bacteria growth. Thus, drum dryers are enclosed in special clean rooms that require special cleaning, clothing from the people working, and regulations.

Figure 2: Drum dryer. Commercial product (5)

To produce the steam that heats internally the drum, the process begins with a boiler, typically fuelled by gas or oil, that heats a large volume of water in a pressurized chamber. This creates steam, which is then stored in the accumulator tank. The steam is then passed through a distribution node, which routes the steam to different processes. The steam is delivered to these

processes at the desired pressure and temperature. The used steam is then sent back to the accumulator tank, where it is cooled and condensed back into water. The condensates from the processes then return to a condensate tank. The condensate tank stores the condensates before the condensates are fed back into the steam generator. This closes the loop and allows for continuous steam production.

1.2 Spray drying

Spray drying is an efficiently used process in the food industry to produce powders and granules from liquid or slurry feedstocks. The process involves atomizing a feed solution or suspension into small droplets that are then rapidly dried in a hot gas stream, resulting in the formation of dry particles. Currently, only a few food industries use it and this food industry in Greece is one of the greatest food industries in Greece that could incorporate it, after evaluating the results of this thesis. Currently, this food industry uses drum drying in one of the factories in Greece.

Some of the advantages of spray drying in the food industry include the ability to produce uniform, free-flowing powders with consistent properties, as well as the preservation of nutritional and functional properties of the feedstock. Hammami and Rene (6) report that spray drying is 4 to 5 times more economical than freeze-drying due to less electricity consumption and short drying times.

Some of the challenges of spray drying in the food industry include the potential for heat-sensitive components to be damaged during the drying process, as well as the potential for the formation of off-flavors and odors due to Maillard reactions and other chemical reactions that can occur during the process.

While each method has its advantages and disadvantages, spray drying is generally considered more sustainable than drum drying for several reasons:

- ***Energy efficiency:*** Energy efficiency: Spray drying is more energy-efficient compared to drum drying. In spray drying, a fine mist of the liquid substance is atomized into a hot air stream, resulting in rapid evaporation, and drying. The large surface area created by the atomized droplets allows for efficient heat transfer, leading to shorter drying times and reduced energy consumption. In contrast, drum drying involves spreading the substance onto a heated drum surface, which requires more energy to evaporate the moisture with the reduced heat exchange area.

- ***Reduced water consumption:*** Spray drying typically requires less water compared to drum drying. In spray drying, the liquid substance is atomized into small droplets that quickly evaporate in the hot air, resulting in minimal water usage. Drum drying, on the other hand, often requires a substantial amount of water to facilitate the drying process

and prevent product from sticking to the drum surface and a high amount of water for CIP (Clean In Place).

- ***Preservation of product quality:*** Spray drying is known for its ability to preserve the quality and characteristics of the dried product. The rapid drying process in spray drying helps maintain the original composition, flavor, color, and nutritional properties of the substance being dried. Also, due to the increased heat exchange area, the temperature at which the food is exposed is lower in order to be dried, resulting in lower degradation and reducing the danger of Mallard reactions. In contrast, drum drying can expose the substance to prolonged heat, which may lead to degradation or loss of certain qualities. Thus, spray drying can offer less damaged food and less food waste.

- ***Flexibility and versatility:*** Greater adaptability and diversity in the handling of substances is provided with spray drying. Heat-sensitive foods like fruits and volatile substances can be dried without much degradation, due to the lower temperature achieved. Those foods would face difficulties or be impossible to be dried effectively with drum drying.

- ***Reduced space requirements***: Spray drying equipment tends to be more compact compared to drum drying systems. This smaller footprint is advantageous in terms of space utilization, especially in industrial settings where floor space is valuable. Drum drying systems typically require larger drying chambers, which can be a limitation in certain facilities.

Spray dryers can be more energy efficient and sustainable than drum dryers when coupled with solar thermal energy. The reason is that the steam needed for drum drying is internally heating the drum and thus energy losses increase. Then this heated drum heats the food. In the spray dryer, there are also losses for the heat exchange of steam to dry air, but the maximum temperature needed is 170°C, which is lower than the 195°C of steam needed for drum drying. In the case of drum drying, there is an already set temperature needed for the steam inside the drum in order to dry the food, while in the case of the spray dryer, the temperature of the steam needed can be decreased by the increased efficiency of the heat exchanger, making it more even more suitable for this application and this is why it is chosen. More of these steps are described in the next sub-chapter.

To propose an efficient and sustainable drying system, the following literature review mentions some solutions to increase the efficiency and the parameters that affect spray drying that could be addressed during the research and development phase.

1.2.1 Spray drying with a two-fluid nozzle

Two-fluid nozzle spray dryers have the capability to generate fine particles, measuring less than 10 microns, from both water and organic solvents and therefore are suggested for efficient

spray drying (7,8). The production of small droplets through atomization is the initial step in achieving the desired particle size, which is further reduced during the drying process. The size distribution of the initial droplets plays a crucial role in determining the final particle size and is essential for any spray dryer simulation. However, accurately measuring the extremely small and rapidly moving droplets produced during atomization has always posed significant challenges. Droplet size has usually been estimated by back-calculating from the final particle size and bulk density.

Kemp *et al.* have undertaken a study on this subject, employing a laser imaging setup at GSK to directly measure droplet size from a two-fluid nozzle (9). The utilized nozzle was a two-fluid nozzle featuring a nozzle insert diameter of 0.7 mm and a cap diameter of 1.5 mm. Typically, droplet size has been estimated by reverse calculation based on the final particle size and bulk density. The findings of this study encompassed the following outcomes, that could be beneficial in the actual implementation of the process of this thesis.

- Increasing gas flow gives higher relative velocity and greater shear forces to atomize the droplets.
- Generally, droplet size increased with increased liquid flow rate, although it did not have the same impact as the atomization gas flow. At liquid flow rates below 0.08 g/s (5 ml/min), there appeared to be a further increase in droplet size.
- The measured droplet sizes are reasonably consistent with those estimated by reverse calculation from measured particle sizes, considering the inherent limitations of error and variation in both measurements. Moreover, the trend of decreasing droplet size and reaching an asymptote with increasing atomization flow is similar in both approaches.

In order to realize the balance in spray dryers, Kemp and Oakley categorized spray dryer models at five levels, and the following results came up (10):

1. Heat and mass balance provide valuable information, particularly regarding the mass balance of water. However, it does not directly pertain to the size of the dryer or its potential performance.

2. Approximate calculations offer an initial approximation of the dryer size and drying time by assuming a basic theoretical model that incorporates constant rate and first-order falling rate drying. Heat and mass balances are commonly used and well-documented (11).

3. Scaling calculations, like integral modes, give overall dimensions and performance figures on scale-up, based on measured drying curves from small-scale or pilot-plant experiments by treating the dryer as a whole.

4. Detailed methods as incremental models, track the local conditions of the solids and gas) as drying progresses, typically as a one-dimensional variation of time.

5. Detailed methods (computational fluid dynamics (CFD)) allow for complex three-dimensional flow patterns or the behavior within a single droplet or particle.

Models at Levels 1 to 3 are categorized as lumped parameter models, which treat the dryer as a whole or as a few large regions. In contrast, Level 4 and 5 models are distributed parameter models designed to simulate particle tracking and localized conditions. These advanced models require more extensive input data, including additional physical properties, and employ more complex modeling techniques. In the case of spray dryers, each droplet and particle undergo individual drying, and their drying behavior is influenced by factors such as size, temperature history, and local air velocity.

Heat and mass balances at Levels 1 and 2 are instrumental in scale-up and production rate calculations. They help determine the dependence of liquid feed rate and solids throughput on variables such as drying gas flow rate, temperature, and solids concentration in the feed. In addition, single droplet drying calculations at Level 2 provide insights into the minimum time required to evaporate a pure liquid droplet without any internal mass transfer resistance.

Regarding the experimental setup considered, it has been determined that droplets with a size of 10 μm or smaller have relatively quick drying and can be expected to exit the spray chamber as dry particles, without taking into consideration the residence time in the chamber (9). Nevertheless, as the initial droplet size increases beyond this threshold, the possibility of incomplete drying to reach the final equilibrium moisture content significantly increases. This highlights the crucial role of atomization since excessively large initial droplet sizes make it challenging to adequately dry all droplets before they leave the spray chamber.

Based on the analysis of droplet size, temperature, and moisture content profiles, it has been concluded that larger droplets require more time to reach the critical moisture content. As a result, crust formation occurs later, and water particles are produced during the same residence time. This happens because once crust formation occurs, the external heat and mass transfer become extremely rapid, leading to the almost instant removal of moisture from the surface. The moisture within the particle are based on steady-state diffusion, transitioning smoothly from constant rate drying to a point where internal diffusion cannot match external mass transfer. The liquid thought inside the particle must then diffuse through the formatted crust to leave, either as liquid or vapor. This transport process is significantly slower than the surface evaporation rate controlled by external heat and mass transfer and operates independently of it.

Kemp *et al.* based on their research have concluded that the final particle size in a spray dryer with a two-fluid nozzle primarily depends on atomization conditions, particularly the atomization gas flow rate (9). However, the liquid flow rate and solids concentration also play a role. Computational fluid dynamics (CFD) simulations of gas and particle flow patterns in two types of spray chambers have revealed the presence of a zone of rapid flow originating from the atomizer. This results in a mean particle residence time of less than 1 second.

Consequently, there is a high probability of particles emerging from the spray chamber with high moisture content, leading to downstream stickiness issues. This is a matter of high significance that should be taken into account when designing the process in detail.

1.2.2 Agent addition in spray drying for increased efficiency

According to Cano-Chauca *et al*. spray drying sugar-rich foods, such as fruit juices, holds a significant economic advantage due to the benefits of transforming these products into a dry form (12). The conversion to a powdered form reduces the volume and extends the shelf life of the products. Long-lasting self-products translate to decreased food waste. However, it is important to note that fruit juice powders possess high hygroscopicity, meaning they absorb moisture from the surrounding air. This hygroscopic nature can lead to issues such as stickiness and difficulties with flow properties found in spray dryers. Proper handling and packaging techniques are crucial to mitigate these problems and maintain the quality and usability of fruit juice powders later on.

To address the challenges associated with stickiness, as mentioned before, and hygroscopicity in powders produced from spray drying, the use of carrier agents like maltodextrin is recommended during the drying process. By incorporating maltodextrin, which has a higher molecular weight, the glass transition temperature of the product is raised. The glass transition temperature is the one that the product starts to have a softer state compared to the one originally had. This helps to prevent stickiness issues and decreases the powders' ability to absorb moisture from the environment. Furthermore, carrier agents play a vital role in protecting sensitive food components. They act as protective barriers, shielding these components from unfavorable environmental conditions such as moisture, oxidation, or degradation. This preservation effect helps to maintain the quality and stability of the powder, improved overall product performance ensuring a longer shelf life, promoting sustainability, and reducing waste (13).

The research conducted by Ferrari *et al.* on the usage of maltodextrin, demonstrated that all the produced fruit juice powders, which have stickiness properties, had moisture contents below 3% (14). With increasing concentrations of maltodextrin, the hygroscopicity of the powders decreased significantly. This decrease can be attributed to the low hygroscopic nature of maltodextrin. These findings confirm the effectiveness of maltodextrin as a carrier agent during the spray drying process. However, it should be noted that excessive concentrations of maltodextrin can lead to a decrease in the quality of the resulting powder. This is because higher concentrations of maltodextrin may dilute the nutrients present in the fruit, compromising the nutritional value and overall quality of the powder. Therefore, it is important to strike a balance in selecting the appropriate concentration of maltodextrin to achieve optimal powder quality while maintaining the desired reduction in hygroscopicity (15). To elaborate on this issue, an innovative solution is presented later.

Furthermore, the inlet air temperature had a significant impact on the hygroscopicity of the powder. Specifically, higher drying temperatures were associated with increased

hygroscopicity in blackberry powder. This means that at higher drying temperatures, the resulting powder exhibited a greater ability to absorb moisture from the surrounding environment. Furthermore, the study observed an inverse relation between hygroscopicity values and moisture content. Powders with lower moisture content demonstrated higher hygroscopicity and this behavior may be explained by the larger difference of water concentration between the powder and the surrounding air, which makes it easier for moisture to be absorbed. It is important to highlight the influence of drying temperature and moisture content on the hygroscopicity of powders when designing spray drying processes like this. Higher drying temperatures and lower moisture content contribute to increased hygroscopicity, indicating a greater propensity for the powder to absorb moisture from the surrounding air.

In spray drying cactus pear juice, Rodrıgues-Hernandez *et al.* observed that the powders produced with higher concentrations of maltodextrin and lower inlet air temperatures exhibited lower hygroscopicity (16). In other words, there was less of a tendency for these powders to absorb moisture from the surroundings. Goula and Adamopoulos discovered that the impact of process factors on the glass transition temperature was characterized as influencing the powder hygroscopicity (17). In the case of spray drying of orange juice concentrate, increasing the inlet air temperature and maltodextrin concentration had specific effects on the powder's glass transition temperature and hygroscopicity values. With increased inlet air temperature during spray drying, the powder's glass transition temperature was raised. This elevation in the glass transition temperature led to lower hygroscopicity values, indicating reduced moisture absorption. As a result, the powder exhibited increased stability during storage, as it was less prone to absorbing moisture from the surrounding environment, increasing the self-life and thus reducing food waste. Similarly, increasing the maltodextrin concentration in the spray-dried orange juice concentrate also contributed to a higher glass transition temperature and lower hygroscopicity values in the resulting powder. This effect can be attributed to the protective properties of maltodextrin, which acted as a barrier against moisture absorption. The particle size distribution resulting from spray drying ranged from 12.52 to 34.18 mm, suggesting that the process effectively generated small particles. Obon *et al.* showed that the spray drying of cactus pear juice yielded an average particle size ranging from 10 to 12 mm (18). On the other hand, the mean diameter of spray-dried acai powder varied between 13 and 21 mm. This comes to show the versatility of the spray dryer compared to drum drying. In spray drying, the ability to adjust the temperature gives the option to the user to dry different types of food as well as to adjust such parameters for the best possible result.

Furthermore, higher inlet air temperatures during spray drying were found to be associated with larger particle sizes. This phenomenon can be attributed to increased swelling of the particles as the drying temperature rises. When subjected to higher drying rates, moisture evaporates rapidly from the particles, leading to the formation of a hard crust. This crust prevents the particles from shrinking during the spray drying process, resulting in larger particle sizes. Conversely, lower inlet air temperatures allow the particles to remain moist for a longer duration, enabling them to shrink during the drying process. As a result, the particle size decreases when the inlet air temperature is lower. In summary, the relationship between inlet air temperature and particle size during spray drying can be explained by the drying rate

and the formation of a hard crust. Higher temperatures lead to larger particles due to limited shrinkage due to initial crust formation, while lower temperatures promote shrinkage and result in smaller particle sizes.

Goula and Adamopoulos showed that the size of spray-dried particles is directly influenced by the size of the atomized droplets, which, in turn, is affected by several factors such as the type of atomizer used, physical properties of the feed solution, and concentration of the feed solids (19). When the viscosity of the feed solution is increased, it leads to the formation of larger droplets during atomization, resulting in the production of larger particles during spray drying. Therefore, the size of the atomized droplets, which is influenced by factors such as viscosity and concentration of the feed solution, directly impacts the size of the resulting spray-dried particles.

The same source reports that when a low inlet air temperature of 140°C was utilized during spray drying, it resulted in the production of particles with a dry and textured surface. On the other hand, when higher drying temperatures of 180°C were employed, the spray-dried particles exhibited smoother surfaces. This observation holds for various products, including cactus pear and milk, that have undergone spray drying processes. The surface texture of the spray-dried particles is influenced by the drying temperature. Lower temperatures tend to promote a dry and textured surface, possibly due to slower evaporation and the formation of a porous structure. In contrast, higher drying temperatures facilitate faster moisture removal, resulting in smoother surfaces with less porosity. Hence, the choice of inlet air temperature during spray drying can impact the surface texture of the particles, with lower temperatures favoring a dry and textured surface, while higher temperatures yielding smoother surfaces. This behavior has been observed consistently in the spray drying of different products, such as cactus pear and milk. Kurozawa *et al*. reported that the shrinkage of spray-dried particles is influenced by the drying rate, which is lower when a lower inlet air temperature is used during the spray-drying process (20). In such cases, the slower drying rate leads to slower water diffusion within the particles. This extended drying time allows for more structural deformation, shrinkage, and collapse of the particles. When the drying rate is slower, there is more time for the particles to undergo internal changes and rearrangements as moisture is gradually removed. Therefore, the drying rate, which is influenced by the inlet air temperature, has a crucial role in the shrinkage of spray-dried particles. Lower inlet air temperatures result in slower drying rates, allowing for increased particle shrinkage due to extended water diffusion time and subsequent structural deformation.

Concerning powder morphology, higher inlet air temperatures during spray drying resulted in larger particles with smooth surfaces. On the other hand, lower maltodextrin concentrations led to the production of smaller particles. The optimal processing conditions for preserving the anthocyanin content and color characteristics of the powder were identified as an inlet air temperature of 140°C -150°C and a maltodextrin concentration of 5% - 7%. These conditions were found to be favorable for maintaining the quality of the powder, specifically in terms of its anthocyanin content. Anthocyanins are important natural pigments that contribute to the color and potential health benefits of food products. The findings highlight the potential

applications of these powders in various food and nutraceutical products, including dry mixes, beverages, desserts, and other food formulations. These findings demonstrate the versatility and commercial viability of utilizing such powders as valuable ingredients in the food industry (14).

1.2.3 A novel spray dryer with freely rotatable propellers

To address the challenges associated with spray drying, a novel design of a laboratory-scale spray dryer has been developed and discussed, which could be a great addition to the proposed system for increased powder yield because it allows for the production of high-quality powdered products without the use of excessive additive agents. This design incorporates a mechanical and aerodynamic manipulation system that aims to reduce the deposition of powder particles on the drying chamber walls and minimize the adhesion of particles to each other. By implementing innovative mechanisms, the system promotes better particle dispersion and prevents the particles from sticking to surfaces, thereby improving the overall efficiency of the drying process. By eliminating or minimizing the need for additives, potential negative effects on the color, taste, aroma, and other quality attributes of the final product can be avoided. This novel laboratory-scale spray dryer design offers promising prospects for improving the efficiency and quality of spray drying operations, providing an alternative solution to the challenges faced in traditional spray drying processes (21). The novel design of the laboratory-scale spray dryer incorporates two units of 3-vane propellers strategically placed within the drying chamber. These propellers serve two main purposes: to facilitate a more homogeneous airflow distribution throughout the chamber and to lower the temperature of the glass wall. By introducing the 3-vane propellers, the airflow within the drying chamber is effectively mixed, ensuring that the hot air is evenly distributed, and minimizing temperature variations within the chamber. This homogenous airflow helps to prevent localized hotspots and ensures consistent drying conditions for the sprayed particles. Additionally, the propellers play a role in lowering the temperature of the glass wall of the drying chamber. This helps to minimize or eliminate the deposition of powder particles onto the chamber walls, reducing the need for constant cleaning and improving the overall efficiency of the drying process. The spraying process in this design takes place in a cylindrical glass chamber with a downwards co-current, two-fluid pressure nozzle atomizer, as proposed in this thesis.

The results in the research of Iik and Yildiz (21), showed an advantage in using a spray dryer with a freely moving propeller, affecting the most important parameters of the final product. The average velocity of the outlet air was 7.7 m/s in the conventional spray dryer and 10.3 m/s in the one with the freely rotatable propellers. The thermal efficiency of the dryer with propellers achieved was higher at 68,97 % compared to the conventional one at 66,72 %, with the highest efficiency achieved with a nozzle of 2.5 mm and an inlet temperature of 200 °C. Although in the suggested case the drying of milk requires a lower temperature, this can increase the thermal efficiency as well as in the cases with other products that require temperatures up to 200 °C. An interesting result was that the higher the size of the nozzle diameter, the higher the efficiency that was achieved was, in both cases. Furthermore, the maximum product yield was 109 g on the conventional and 119 g on the novel one, at the same

nozzle size and at 140 °C. This could be a great fit in the designed spray dryer and experiments could take place to find out the results.

The amount of milk produced in the aforementioned report, which is the product used at this thesis, was reported to increase as the nozzle size increased and the temperature decreased. Thus, in the process design, the lowest possible temperature will be set for the milk. Also, the developed spray dryer achieved less adherence of the powder particles on the walls due to the propeller rotating the power in the airflow direction, aiding the cleaning afterward as well. An important advantage reported with the addition of the propellers concerns the minimum and maximum moisture content in milk experiments, with the conventional having a minimum of 2.51 % and a maximum of 3.71 % moisture while in the one with the propellers, it came up to was minimum of 1.25 % and a maximum of 2.99 % of moisture, showing better moisture reduction with this system. Therefore, this could be a great addition to the spray dryer, when implementing the proposed system in the food industry, during research and development.

Table 1: Parameters affected during spray drying and their result in production

Parameters	**Result**
Increased gas flow	Increased relative velocity
Increased liquid flow	Increased droplet size
Droplet size <10μm	Dries relatively quickly
Increased droplet size	Increased drying time
Increased nozzle diameter	Increased thermal efficiency
Drying rate and droplet drying time	Mostly depend on initial droplet size
Addition of maltodextrin	Decreased hygroscopicity
Addition of maltodextrin (only)	Decreased particle size
Increased drying T (+maltodextrin)	Increased hygroscopicity leading to higher stability under powder storage
Increased moisture (+maltodextrin)	Decreased hygroscopicity
Increased drying T (+maltodextrin)	Increased particle size
Increased size of spray dried particle (+maltodextrin)	Increased viscosity
Increased T (+maltodextrin)	Smoother surface (up to 180 °C)
Implementation of freely moving propeller in spray dryer	Increase in average air velocity by 2,5 m/s Increased thermal efficiency by 2,2 % Increased in mass yield by 10 %. Decreased adherence. Decreased moisture.

2. Energy usage

The availability of energy is crucial for the economic, social, and national development of every nation. This is more profound in the past 2 years with the energy crisis taking place in Europe. Meanwhile, as the world's population, industrialization, and urbanization continue to grow, there is a rapid increase in global energy and electricity consumption. Unfortunately, conventional energy sources are depleting and contribute to harmful emissions, which brings significant challenges in providing a sustainable and clean energy supply for the growing population (22). In comparison to global population growth, energy consumption is not increasing linearly but exponentially, and in conjunction with the COVID-19 pandemic, in 2021 the global coal demand almost reached peak values of the past, despite the effort for cleaner and sustainable energy (23).

Preliminary 2022 data from IEA predict that it will reach an all-time high. In the meantime, oil and natural gas demand, and thus pricing, have almost picked as well, making the energy need worldwide more profound than ever. In the meantime, the usage of fossil fuels contributes negatively to the target to achieve a limit of a global rise in temperature of 1.5 °C to 2 °C. Thus, the consumption pathway of renewable and conventional energy sources plays a crucial role in sustainable development, serving as critical indicators of resource use and environmental impact. Presently, 80 % of the global primary energy supply comes from depleting fossil fuels such as coal, natural gas, and liquid petroleum, which emit significant Greenhouse Gases (GHG).

As such, industrialization has become a significant driver of the increasing trend in energy consumption. The industry sector, which consumes the most energy globally (38 %), largely relies on non-renewable energy sources like fossil fuels and natural gas (24). This dependence on hydrocarbons has led to a surge in GHG emissions, exacerbating the impact of climate change (25).

2.1 Energy consumption in industries

Industrial heat production processes have a considerable share of Europe’s pollution due to the emissions produced from the current fossil fuels used, including GHG and air pollutants.

The Industrial Emission Directive (IED) targets the protection of people’s health and the environment’s sustainability, by reducing the emissions across EU, making use of the Best Available Techniques (26). The IED, being well aligned with the clean energy for all European package strategy aims to increase the energy efficiency and the renewable energy share in industrial processes. The waste heat sources exist in all industries with a total amount of 300TWh/year in the EU, while the European industrial sector is one-quarter of EU28’s final energy consumption, with 260 Mtoe in 2019 (27). The existence of waste heat could be used for district heating, well coupled with solar heat from concentrated solar thermal collectors. During this process design, there will be two waste heat regeneration points.

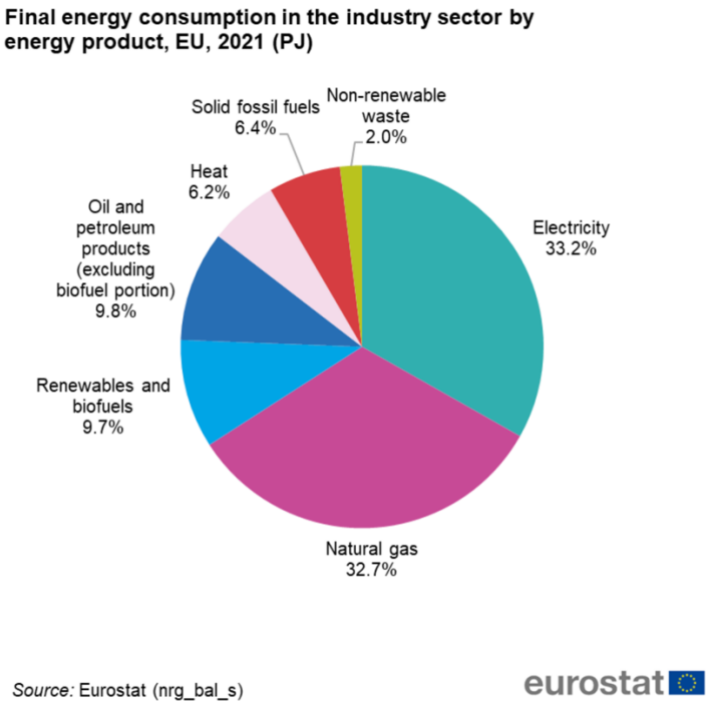

Figure 3: Percentage of energy source consumption by industries(28)

The figure above represents the distribution of final energy source consumption in the industrial sector for 2021. It can be seen that the energy usage of renewable sources in industries is still low. In the meantime, the most heat-intensive industries are the chemical and petrochemical, non-metallic minerals, paper, pulp and printing, and the food industry. Since more than two-thirds of the total energy consumption in industries in the EU, and half of this process heat demand is at low to medium temperatures (i.e., lower than 400 °C), there is a high potential in the application of solutions such as solar thermal and photovoltaic combined with high-pressure heat pumps in that sector.

Furthermore, the above figure shows for each temperature range the energy consumption share for the industrial heating process. It can be observed that in the food industry, 75 % of the processes take place below 200ºC.

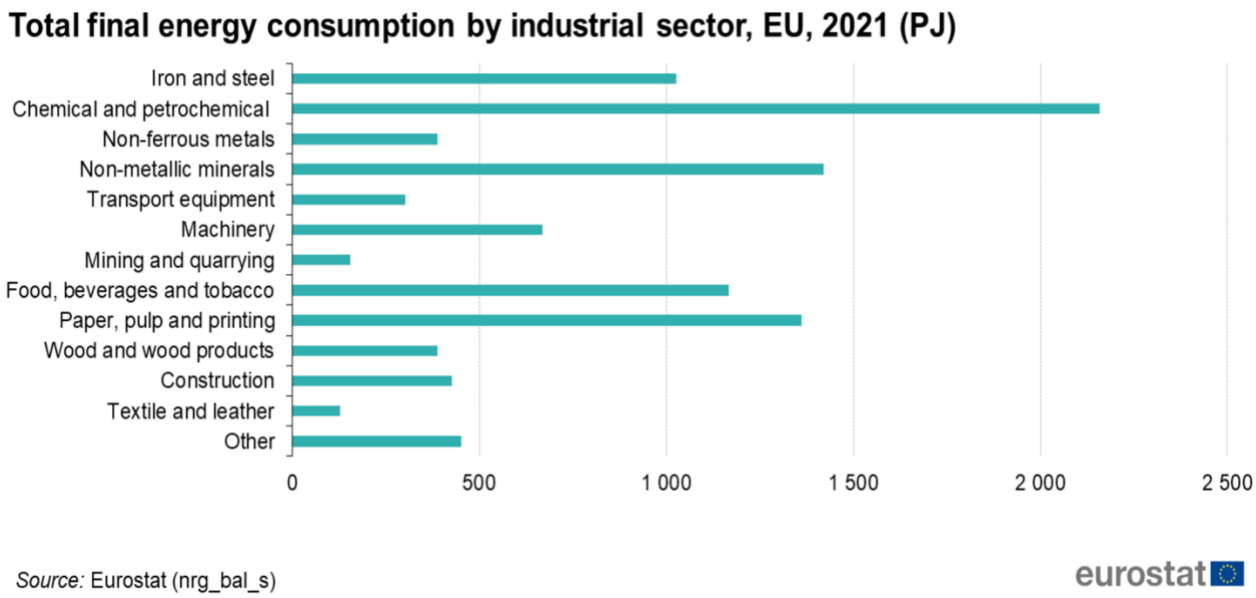

Figure 4: Types and temperature range needs in different industries (29)

Thus, to mitigate the effects of pollution and address the challenge of resource depletion, the industry sector must integrate clean and sustainable energy sources. The industry can adopt energy-efficient methods, and incorporate renewable energies, particularly solar energy, which has significant potential for reducing CO_2 emissions due to its availability and abundance (30). To do so, there are various ways commercially available and under development constantly, including solutions like photovoltaics, solar thermal, wind turbines, and biomass, which subsequently can undergo several processes in order to be used by the end user or stored under electrochemical, mechanical, thermal and chemical forms.

This thesis aims to increase environmental sustainability in the food industry to achieve decreased GHG emissions. It has been established that spray drying differs from drum drying, and it is examined how energy usage can be decreased. In order to increase the impact of this and make it more sustainable, the acquisition of clean energy for spray drying can make it run fossil free to produce food. Solar power can be very beneficial for a specific process. Solar energy can be harnessed in two ways: direct conversion to electricity through photovoltaic cells, and thermal conversion using solar collectors (31). State of the Art commercially available photovoltaics offers a maximum efficiency of 20 % to 23 %, which will then be lowered if used to heat water or air, due to the subsequent energy conversions. On the other hand, solar heat collectors can convert solar energy to heat in the form of pressurized water or steam with an optical efficiency of over 76 % operating on average with efficiencies above 50 % converting solar radiation directly into heat at different temperatures. By implementing these methods, the industry sector can contribute to the reduction of air pollution levels as well as a significant reduction of GHG emissions towards a sustainable energy future.

2.2 Advantages of CSP installations

CSP plants are one of the most researched sustainable means for energy generation because of being able to produce both heat and electricity, can have affordable thermal energy storage (using molten salts for instance), a non-hazardous operation, and a long-term operation experience (since the 1990's). The technology by offering on a small or large scale, hot water, direct steam as well as electricity when found in the form of solar thermal electricity, has the potential to contribute to a cleaner energy sector since when coupled with storage solutions, can run throughout the whole day having the capacity to operate 24/7 which makes it a very valuable asset of the electricity power plant system (32).

2.3 Status of CSP plants

Throughout the world, the number of CSP plants has started to increase and in 2019 the production reached 6451 MWe, with Spain and the United States being the leaders, while China, Morocco, and South Africa are the upcoming countries (33). In Figure 6 the global installed capacity in 2022 is portrayed. It is observed that in 2018 and 2019, the installed capacity vastly increased from 5000 MWe to 6500 MWe by introducing new industry stakeholders in China, Morocco, South Africa, and Israel (34,35).

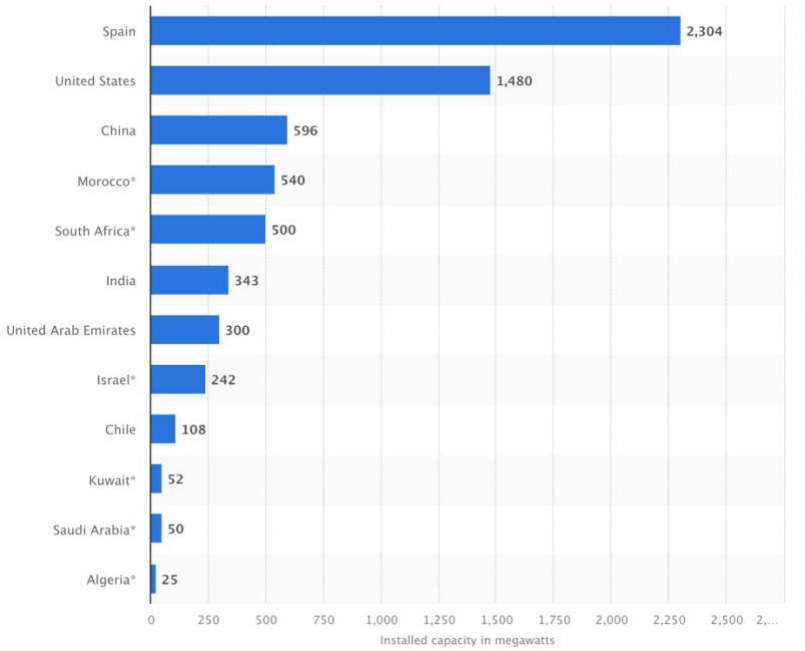

Figure 5: Global installed capacity of CSP (36)

The majority of installations exist in Spain, USA, Mexico, China, Morocco, and South Africa. Southern Greece, where the following concentrating solar thermal for industrial processes simulations will be done is a country with great radiation and thus potential, as displayed from SOLARGIS.

Figure 6: Solar radiation in Greece (37)

SolarPACES and Chemical Energy Systems have compiled the data displaying the share of and the power of CSP plants production across the world and the exact locations respectively up to July 2022 which are either operational, under construction, or in development. CSP technologies include concentrated solar thermal collectors, linear Fresnel reflectors, power towers, and dish systems.

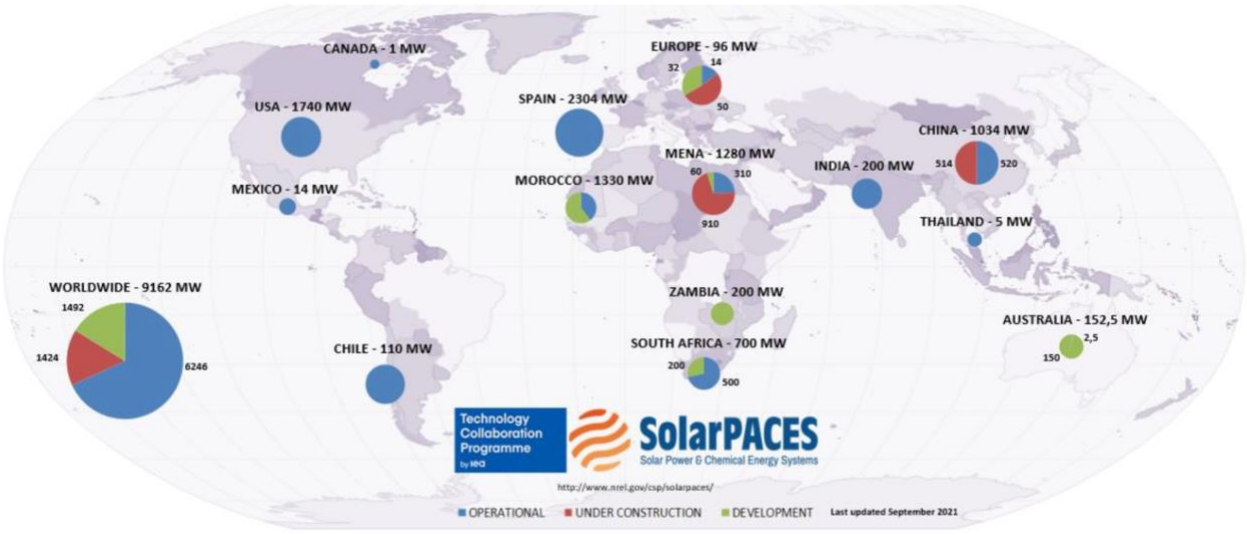

Figure 7: Share of CSP plants in the world (38)

The following figure shows the location of each CSP plant throughout the world.

Figure 8 Locations of CSP plants (38).

2.4 Types of collectors

In order to choose the solar heat technology to cover the needs of the spray drying solution in the food industry, the different categories are analyzed.

2.4.1 Flat plate collector

The flat plate collector (FPC) is one of the simplest type of collectors that take advantage of solar energy by using a glazed-covered black panel, enabling the solar light to penetrate and get absorbed by the plate, in order to generate heat. The absorption takes place in highly conductive metallic sheets made from copper, aluminum, or steel, with a coating on top that maximized the absorption. In more detail, the thermal energy generated is transferred to the tubes that contain a fluid (water, antifreeze, or air) to carry the heat, which is responsible to transfer it to cover needs immediately or to be stored (39). FPCs have a similar theory behind them to PVs, and similarly, by being flat they do not exploit throughout the day the whole radiation, which is the direct and diffused (39). Commercially available FPCs achieve temperatures in the range of 30-80°C, which is protected from heat losses with thermal insulation on the casing and with the glass cover (40) (41). There are cases with special coating where the stagnant temperature can reach higher temperatures. Figure 10 shows the construction and components of an FPC.

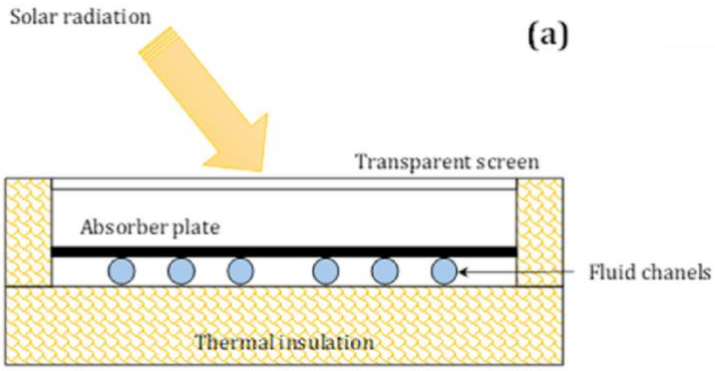

Figure 9 Flat plate collector structure. *Licensed from Elsevier (42)*

For FPC there is a possibility to incorporate a vacuum in its interior, achieving higher efficiency due to the reduced conduction and convection losses, as well as less installation area compared to the simple FPC (43).

2.4.2 Evacuated tube collector

The Evacuated Tube Collector (ETC) uses glass tubes that contain an inner U-shaped tube or one tube, which is covered by a selective absorbing layer, while between the inner and outer tubes, there is a vacuum sealing (40). The generation of vacuum aims to minimize the conduction and convection heat losses, thus enabling the ETC to work at higher temperatures than FCPs. The higher thermal efficiency achieved can reach temperatures up to 200°C, compared to FPCs, while still offering a low-cost (44). The technology offers two variations, the heat pipe ETC and the direct flow ETC. The former is based on an evaporation-condensation cycle, where solar radiation vaporizes a volatile fluid, leading its vapor to the top of the tube (40). The condensed vapor then releases latent heat to the system, becomes liquid, and returns to the bottom, completing one cycle and then repeating.

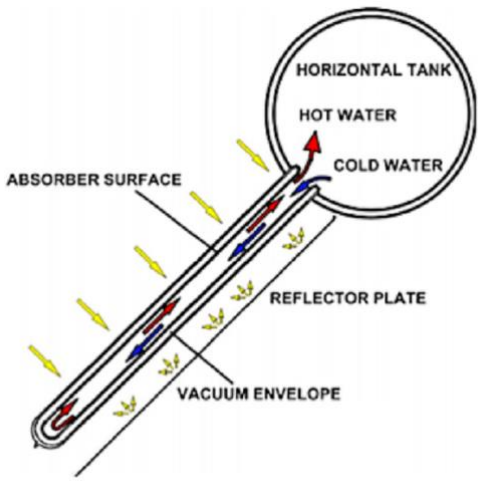

Figure 10: Evacuated tube heat-pipe collector. *Licensed from Elsevier (42)*

The second type of ETC is the direct flow ETC, where the radiation after passing through the vacuum, comes in contact with a U-shaped tube, containing a circulating fluid, which enters cold and is heated up by the incoming radiations. Similar to the former case, the U-shaped tube is covered with a highly conductive selective coating, boosting the heat transfer and minimizing the radiation losses (39).

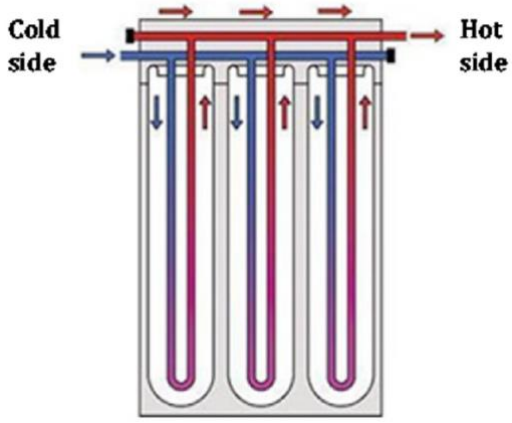

Figure 11: EPC U-shaped. *Licensed from Elsevier (42)*

2.4.3 Compound parabolic collectors

Compound parabolic collectors (CPC) have two parabolic surfaces with the same center with a cover of reflective material. In the center of the parabolic surfaces, there is an absorbing tube that captures the solar radiation and heats the inside passing fluid. The fact that there are 2 surfaces, allows the collector to capture all the incident radiation over a wide range of angles, as well as some diffused radiation, by leading all the radiation eventually to the concentrating tube (45). CPCs achieve temperatures that combined with evacuated tubes, the temperature outcome can be up to 180-200°C (46). Figure 13 shows a CPC schematic representation of this where the two parabolic surfaces concentrate solar radiation in the absorbing tube.

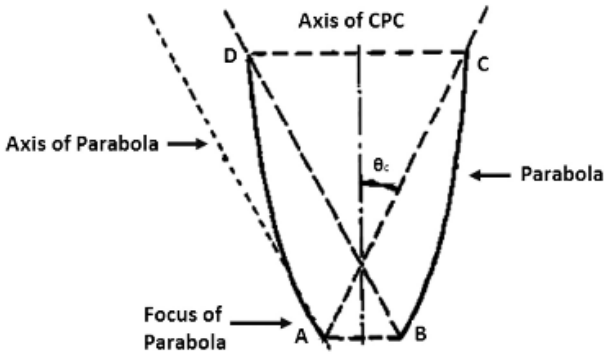

Figure 12: Compound parabolic collector *Licensed from Elsevier. (47)*

2.4.4 Solar Parabolic Dish system

In Solar Parabolic Systems (SPD) there is a point-focus dish collector with a diameter of 5 m -10 m that reflects the incoming radiation to a receiver at the focal point while following the sun with a two-axis system. For efficient energy conversion, a Stirling/Brayton engine is placed, which is a heat engine operating with cyclic compression and expansion of air or other gas at different temperatures, with an electrical generator to exploit the concentrated heat (48). The temperature range is 750 °C -1500 °C, offering very high temperatures compared to other types of CSP and the surface area is 40 m^2-120 m^2 and the surface is highly reflecting and made of aluminum with a coating of glass or plastic (49). Furthermore, the fact that they are not connected, in comparison to parabolic trough collectors, makes them more modular and allows the installation of units independently or in the form of solar parks (45).

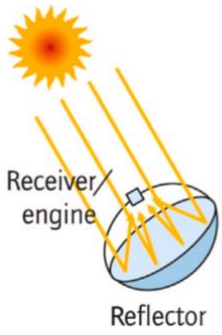

***Figure 13 Solar parabolic dish**. Licensed from Elsevier (50)*

2.4.5 Linear Fresnel collector

The Linear Fresnel Collector (LFC) consists of many reflecting mirrors that aim to a stationary absorbing tube, including a fluid to be heated. The working principle is that solar radiation arrives at the reflectors, which then emits it to the stationary tower to heat the included fluid. To achieve higher efficiency, LFC can include tracking systems if not placed like strips and mounted on flat ground. The principal is similar to a PTC divided into pieces but without the parabolic shape of the mirrors (45). In comparison to PTCs, the LFC technology is simpler and thus easier to implement and construct but sensitive to shading and occasionally limited due to the shading between each other (51). The operating temperature is in the medium range of 60°C to 250°C (52).

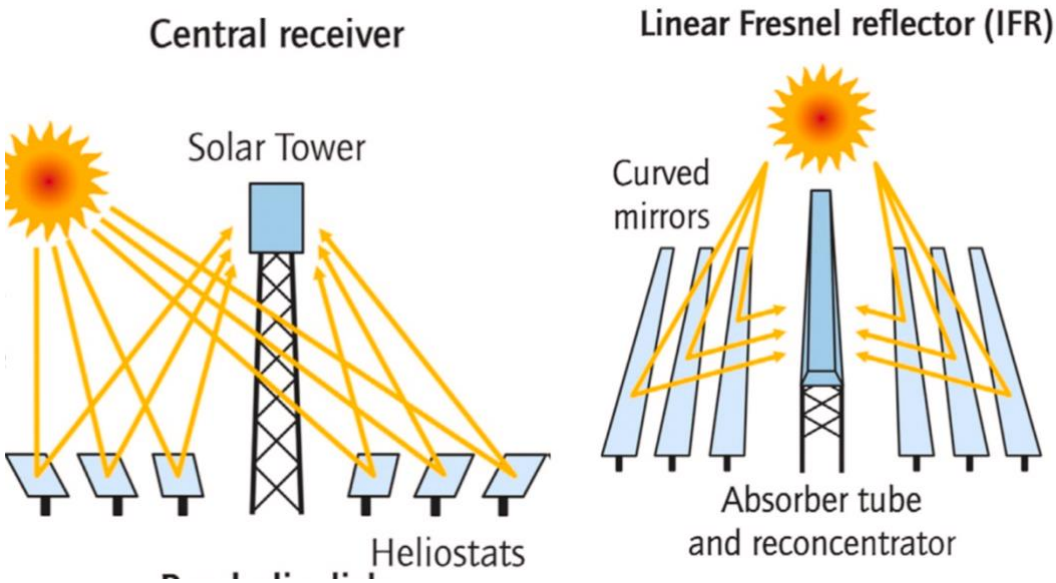

Figure 14: Central receiver and Linear Fresnel reflector structure. *Licensed from Elsevier (50)*

LFC can also be coupled with steam turbines, where the circulating fluid is heated up in the tower and then guided in a simple Rankine cycle, to be expanded and generate electricity (53). Since there are many reflectors and one receiving tower, the capacities are high, ranging from 10 MW to 200 MW, achieving an efficiency of above 70 % (54).

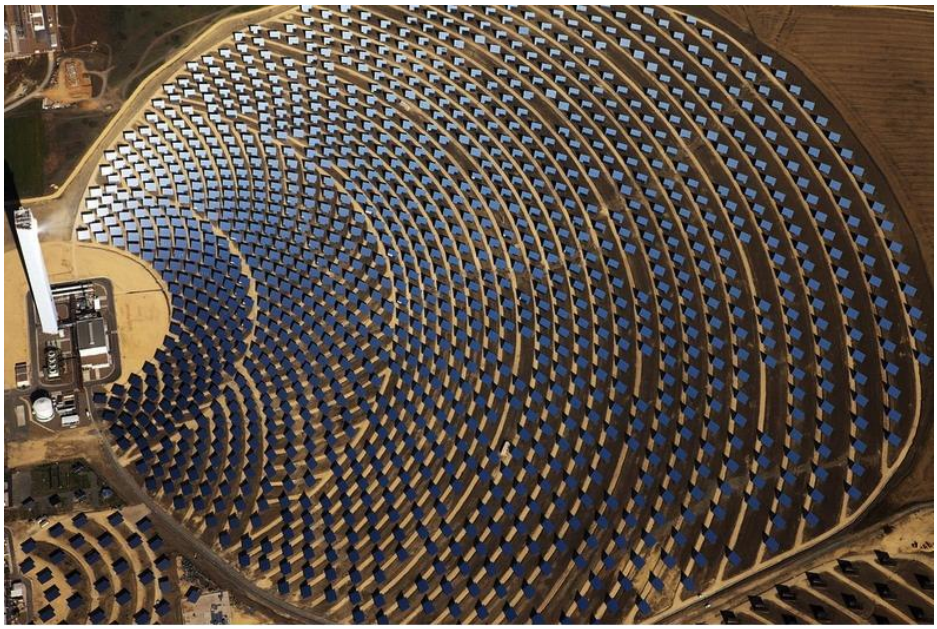

Figure 15: 11MW in Seville, Spain (55).

2.4.6 Parabolic Cylinder Collector/Concentrated solar thermal collectors

The Parabolic Cylinder Collector or Parabolic Trough Collector (PTC) has a parabolic metallic-shaped sheet that reflects and concentrates the incoming radiation to the receiving tube

in point zero of the parabola, called the focal point. They are constructed of a metal casing including the reflective sheet, the receiving stainless-steel tube with a heating fluid like water or oil, and a hardened glass to protect them from harsh weather conditions while being shelf cleaning and anti-reflective.

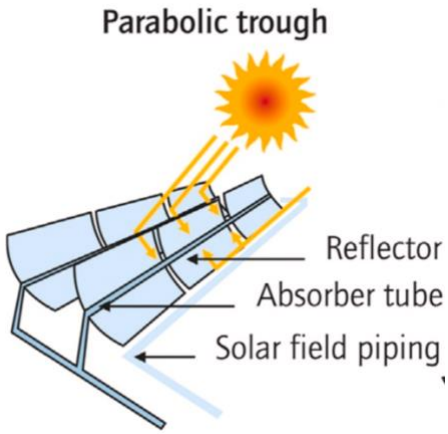

Figure 16: PTC collector and receiver. *Licensed from Elsevier (50)*

The stainless-steel absorbing tube is covered by a selective coating that allows the radiation to be absorbed but limits the convection heat loss from the inside to the outside part. These collectors move throughout the day with a sun-tracking system to follow the sun to maximize the radiation capture and always point the incoming radiation to the focal line. (56,57).

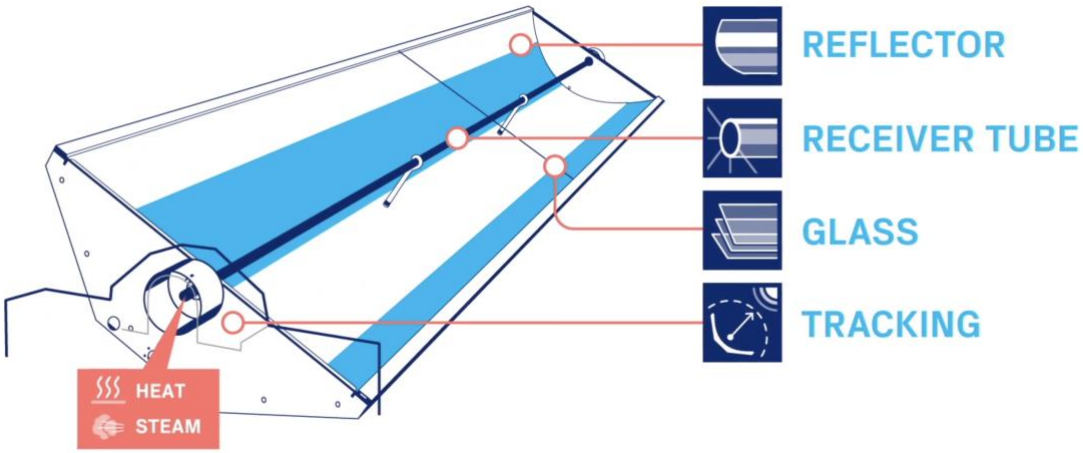

Figure 17: PTC with 1 axis tracking from the manufacturer Absolicon (56)

PTCs can achieve temperatures in the range of 150 °C to 400 °C in the case of having a big aperture area (45). Medium PTCs that are used in industries operate in the range of 50 °C to 160 °C, with Absolicon's medium PTC having the highest commercial optical efficiency of 76.4 %, which is the maximum efficiency of the conversion of incoming radiation to heating (56). One of the most important advantages of this already-matured technology is the direct production of steam for industries, making it possible to generate hot water, pressurized hot water and steam up to 160 °C and 8 $x10^6$ Pa (56). Thus, it is very beneficial for steam-

demanding industries that currently produce steam using fossil fuels because the alternative of using PV to heat water and produce heat will have an efficiency of a maximum of 25 % from the PV electricity generation.

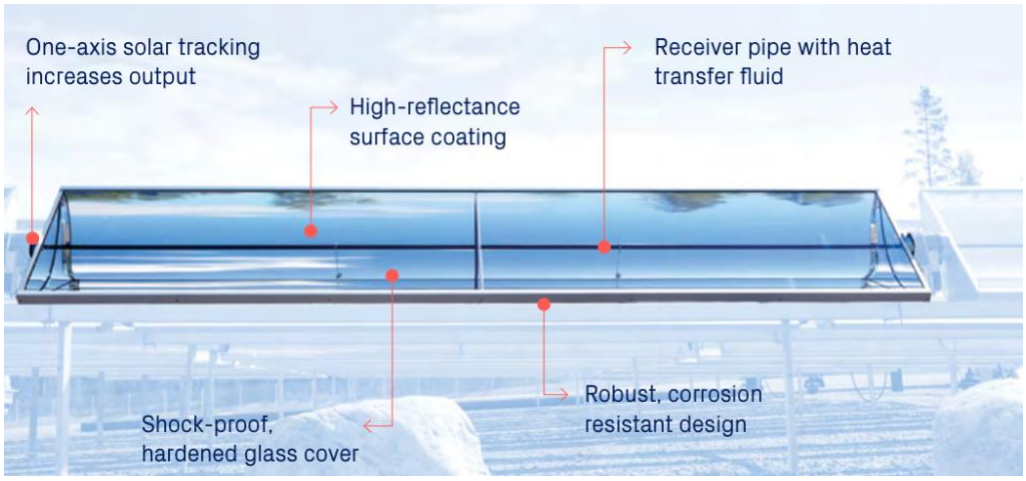

Figure 18: Absolicon's parabolic trough collectors for direct steam generation

In order to achieve higher temperatures in steam production, some manufacturers have developed new designs as is the case of the Absolicon T160 collector, which is the most efficient certified concentrated solar thermal collector in the market in its category. Nevertheless, this collector has a limited maximum temperature that it can efficiently reach (160°C). Thus, Absolicon has been making efforts to further develop a new collector that would be able to reach up to 200 °C. To that end, the conceptual idea (geometry, materials, manufacturing), and initial experimental proof of concept has been developed for a new collector (T220). Absolicon in collaboration with MG Sustainable aims to further develop the design of the collector through extensive simulation and laboratory work to determine the best performing (technically and economically) collector design to be prototyped and tested at the collector level and demonstrate its capabilities at an operational environment.

PTC technology is mature and spread throughout the world with various installations in industries and four production lines in Sweden, China, and two new upcoming in Egypt and Canada.

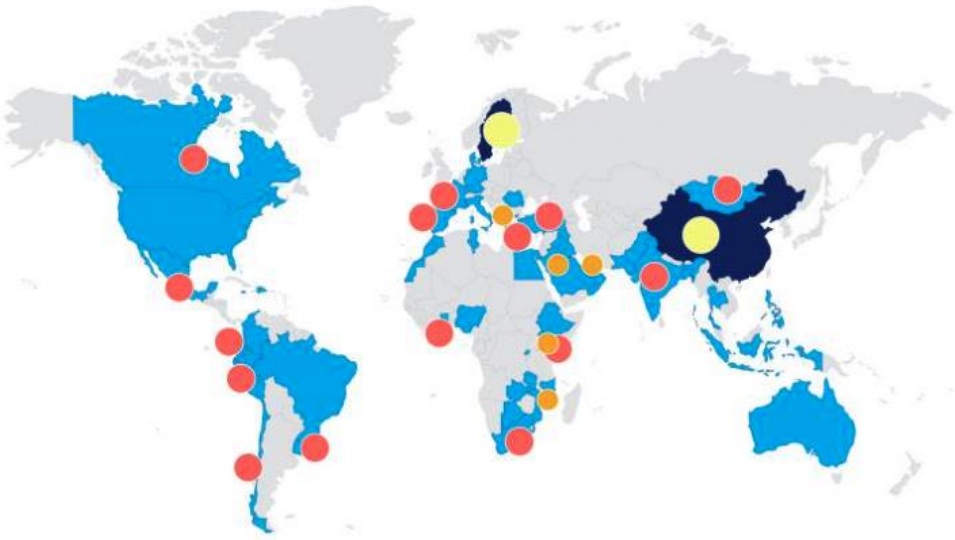

Figure 19: Absolicon's installations and production lines worldwide (56)

2.5 Direct steam generation

PTC among the CSTP technologies is the most proven and commercially available for industries (58). The process of direct steam generation (DSG) within a PTC absorber tube involves a two-phase flow boiling phenomenon and can significantly reduce the cost of electricity produced by solar thermal power plants. As such, it is crucial to examine the thermo-hydrodynamics of flow boiling in horizontal tubes. Accurately predicting the type of flow regimes occurring in the receiver is necessary as it significantly impacts the thermal efficiency of the PTC. In PTC there are three ways to manage fluid circulation, a) once-through concept where the fluid passes once through the tube, b) recirculation of the heated fluid, and c) water injection in the system (59). In 1995, a complete R&D program, called DISS (Direct Solar Steam) project, was initiated to investigate the technical and commercial feasibility of the DSG process. This project included two additional objectives:

3. The development and usage of improved components for concentrated solar thermal collectors (e.g. new lower cost absorber pipes and better optical and thermal properties; sun tracking systems with higher accuracy; new mirrors, etc.),
4. The improvement of the design of the solar park and its coupling to an industry.

The results of the DISS project suggest that it is possible to use Direct Steam Generation (DSG) in Parabolic Trough Collectors (PTC). The researchers behind the DISS project gained

valuable knowledge which led them to create a non-commercial solar thermal power plant project called INDITEP (60). They used the technical and operational experience they gained from the DISS and INDITEP projects to design and set up the first-ever commercial stand-alone 5 MWe solar power plant that uses DSG in Kanchanaburi, Thailand, in 2010-11. The solar power plant is currently being operated by Thai Solar Energy (61).

Flow pattern maps have been utilized to predict the flow regimes at various mass velocities and vapor quality for different operating pressures. Based on the observations made, it has been determined that stratified flow (equal layers of steam on top and liquid on bottom on a horizontal tube) and stratified wavy flow(similar to stratified flow bow the two phases found in waves between them) occur at low mass velocity (between 100 kg/m^2 to 400 kg/m^2), whereas bubbly flow(steam bubbles in the liquid) is observed at very high mass velocity (around 7000 kg/m^2). To achieve annular flow in a DSG collector, it is necessary to maintain high mass velocity (above 400 kg/m^2 at an operating pressure of 100 $x10^6$ Pa). When higher mass flow rates and operating pressures are required, a solar field consisting of several collectors with a longer length is proposed (62).

The DISS project examined the three fundamental DSG alternatives, namely Once-through, Recirculation, and Injection, in actual operating conditions. The most significant conclusion drawn from the project is the confirmation that the direct generation of solar steam is possible in parabolic trough collectors with horizontal absorber tubes. The project has collected valuable knowledge and experience, and design tools for commercial DSG solar plants have been developed, representing a significant advancement in the development of this emerging technology. DSG is a promising choice for creating cost-effective solar thermal power plants that use parabolic trough collectors (63). The three DSG methods were compared at the end of the project using all the experimental data, and it was determined that recirculation was the most practical alternative for commercial use in terms of both technical and economic factors. The use of tiny, inexpensive water/steam separators was made possible by test findings demonstrating the Recirculation process's high stability even at low recirculation ratios.

2.6 Emissions saved

The usage of solar concentrated energy promises decreased emissions for various industries. In order to quantify and demonstrate the reduction of CO_2 emissions and show its impact by using concentrated solar thermal collectors from Absolicon compared to oil in 25 years, as is the lifetime of concentrated solar thermal collectors, some industrial cases have been studied, in comparison to using oil as a fuel. The data for the consumption of each industry have been provided by Absolicon and the calculations have been done using the online Absolicon simulator tool. For confidentiality reasons, the exact location of each industry is not displayed.

Table 1 Emissions saved by implementing only solar thermal parks in various industries in Europe

Type of industry	Location in Europe	Consumption for steam production [MWh/year]	Temperature needed [ºC]	Apperture area for 50% need coverage [m^2]	Emissions saved for 50% need coverage [ton CO_2]	Apperture area for 100% need coverage [m^2]	Emissions saved for 100% need coverage [ton CO_2]
Brewery	South	860	100	661	3605	1322	7209
Brewery	North	91	100	176	386	352	772
Brewery	South	3400	150	3436	13617	6828	27059
Brewery	Central	117	100	298	465	396	930
Cosmetics	South	163	105	110	636	220	1325
Manufacturing	South	1460	115	1145	5893	2291	11791
Pharmateutical	Central	5500	130	8106	22166	16035	43848
District heating	North	1000	120	2115	3984	4229	7966
Chemical	South	390000	160	35154	156281	71586	318243
Ceramic	South	35000	160	2907	14053	5815	28111

3. Methodology

3.1 Steps followed

To write this thesis report about a novel process in the industry, various steps have taken place. For a start, the identification of the current situation in the energy market and food industry was done. Then, an initial contact with the company Absolicon took place, which provides a very novel product; concentrated solar thermal collectors that generate steam directly. This technology can fit the food and milk industry very well because the food industry works in low to medium temperatures and needs steam. It is chosen among the other solar solutions because it provides steam directly with an optimal efficiency of 76.4 %, while it is small and light (50 kg/m^2), making it easy to be installed on small or large scale on industries' roofs or fields. Although photovoltaics and photovoltaic thermal panels could be used, the efficiency of commercial products is in the range of 20 %-23 % for electricity production, which would then undergo through more conversions like for heating the air to 160 °C, which is very energy consuming, resulting in a lower efficiency. Photovoltaic can be used to cover the pump's needs, which is what is planned in this case.

Then, many visits took place to the specific food industry that produces milk powders, to discuss the current process, the complications, the future plans, and the proposed spray drying technology. It was then decided to extract data from the current process and design a process including spray drying and a concentrated solar thermal collectors field for direct steam generation. To perform calculations and design the spray drying process, there was a literature review to decide the operating conditions and assess various parameters.

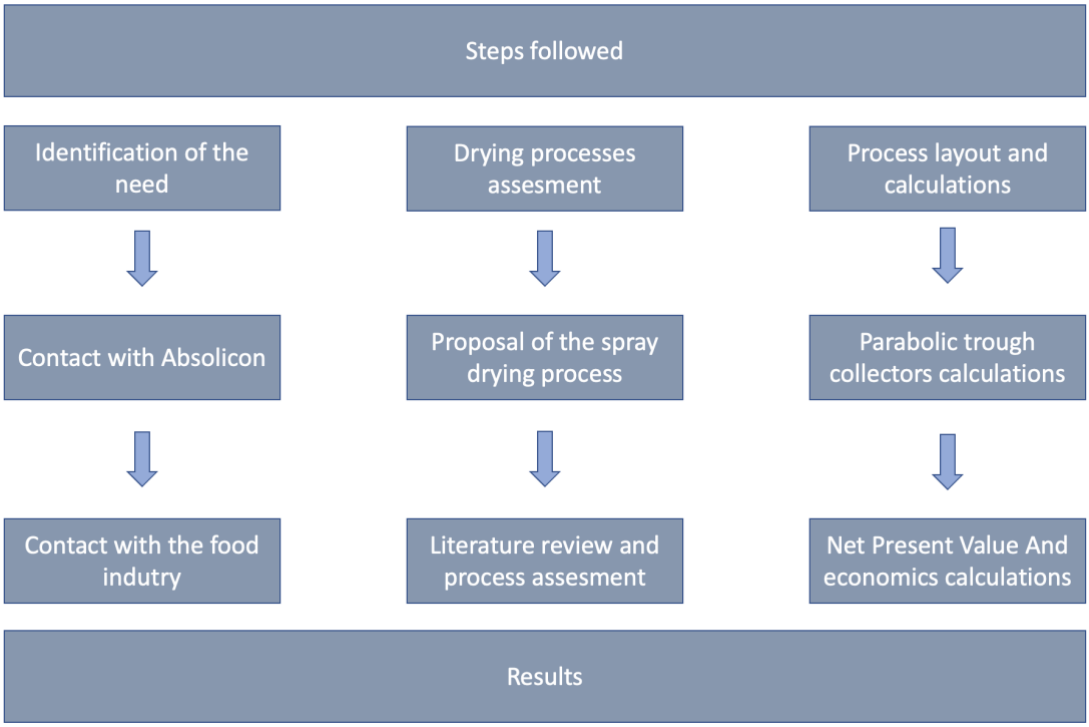

Figure 20: Methodology steps followed

In the specific food industry investigated, there is a need to produce food powder for home and commercial use in an energy-sustainable way. In order to achieve this, the spray dryer, as discussed, is going to be deployed. To accomplish a higher efficiency, maltodextrin, and a freely moving propeller could be used as an addition to the proposed system in the facility to further increase the efficiency.

The product that is going to be dried in this case will be milk, which has an 87 % water content (64). The goal is to produce infant powder, which with the addition of water can become milk or cream. With the same process, other dried foods can be obtained, such as dried dairy products, whey protein powders, or infant food. To calculate the conditions of each step, back-track calculations will be made, starting from the data at the spray dryer acquired from references, continuing to calculations at the heat exchanger, to the solar heat collectors, and then at the air regeneration cooler.

3.2 Spray drying process steps

Since the spray dryer has not been yet installed in the industry under discussion, the conditions of it will be based on references with experiments on actual commercial products. Starting from the spray dryer, Schmitz-Schug et. al have tested various inlet and outlet temperatures as well as product mass flow rates while keeping the sprayed dried air volume constant (65). This work is very insightful since it is done in laboratory and pilot scale and repeatable results can be extracted for the calculations. The spray dryer used was the Production Minor™ by GEA Niro. GEA is a very respected and well-known industrial machine producer in the market of food industry machines and therefore this machine could be employed in the industry by being commercially available. Thus, the suggested procedure can be implemented in more food industries and increase the environmental and economic impact.

Based on these results, the air inlet temperature is set to 160 °C in order to dry the milk mixture sufficiently. The aim is to produce an infant formula, which based on HACCP (Hazard Analysis Critical Control Point) must be a very low-risk food and well-checked. One of the most important parameters when preserving food is water activity. In order to store food and prevent microorganisms from growing, the water activity should be below 0.6, but every microorganism has its limit. Water activity (a_w) is the 'free' water is the food, which is not captured by the cells and thus can be used by the microorganisms to grow. In more detail, it is the ratio of the vapor pressure in a food (P) to the vapor pressure of pure water (P_o). It reviles the tendency of water to move from the food cells into the cells of microorganisms that may be present.

$$aw = \frac{P}{Po}$$

In order to achieve a safe to store final infant powder and decrease the chance of Mallard reactions, where the food becomes brown due to enzymatic reactions, a low water activity of may be chosen (66). Cheng et.al have reported that a_w=0.11 is recommended for protein-rich powders to minimize browning and a water activity of around a_w=0.33 is preferred when lipid

oxidation is the key factor of choice, which determines the shelf-life, corresponding to lipid-rich powders (67). After this value, the water content increases exponentially. Based on the pilot test of Iris Schmitz-Schug et.al, the water content increases vastly compared to a water activity of 0 to 0.04, while for a water activity of 0.04 to 0.33 the water content falls in the range of 4 % to 6 % (65). Therefore, a water content of 4 % to 6 % will determine the conditions of the inlet and outlet at the spray dryer.

In more detail for the spray dryer, the feed will be transferred from the feed tank to two fluid nozzles. Compressed air will atomize the feed, which will then be evenly sprayed into the drying chamber. The process air will be filtered and heated before being introduced to the drying chamber through an air disperser. Once the atomized feed meets the hot process air, water evaporation will occur immediately, causing the feed to dry and become powder that drops to the bottom of the drying chamber. The powder will then be cooled in a specially designed static fluid bed located at the bottom of the spray drying chamber. Any discharged fines will be exhausted to a cyclone and then to a bag filter for proper collection. The spray drying chamber comes equipped with a CIP device for cleaning, while other parts will require manual dismantling. The capacity of water evaporation per hour and the temperature depends on the temperature and operation conditions.

The atomizing system consists of a co-current two-fluid nozzle which is located in the center of the chamber roof, spraying vertically towards the bottom. The nozzle head includes a feed tube and a compressed air tube. A flow meter and pressure gauge keep the values between the set values.

The static fluid bed air heater can be electrical to obtain heated air, or it can receive heated dry air directly, after being heated up by concentrated solar thermal collectors. The drying chamber system has many points for powder discharge, and being in the food industry it has a sanitary design, while the process gas disperser in the chamber roof is easily dismountable for cleaning. The exhaust and powered discharge system is responsible then for the effective separation of the powder and the remaining process gas through a valve and then into a powder container.

Figure 21: Laboratory scale spray dryer with a capacity of powder yield up to 5 kg/h.

3.3 Heat exchangers steps

During this process, the steam will heat up the incoming air to produce dry air for the spray dryer. The energy needed to heat fluids and exchange heat, is found from the equation:

$$Q = m \cdot Cp \cdot \Delta T \qquad (Eq\ 1.)$$

where:

Q= energy rate required to heat up the air in kW=kJ/s
m= mass flow rate in kg/s
Cp= specific heat capacity kJ/kg °C
ΔT= temperature difference in °C

The outlet of the steam, being a condensate, will then go to heat up milk in a pasteurization process, which is also very energy-consuming. Then, it will be directed back to the process and through the second heat exchanger, after the spray dryer. At this point, the outlet of the spray dryer will heat the incoming supply of water, acting as a waste heat stream. This has the advantage that there is preheated supply of water going to the concentrated solar thermal collectors, thus reducing the energy required to be heated, while decreasing the temperature of

the outlet of the spray dryer, meaning that more heat can be absorbed from the steam of the collectors, without creating a temperature cross in the air-steam heat exchanger. The temperature cross is the condition at which the hot stream outlet is lower than the exit of the cold stream outlet (Figure 22). This affects the heat exchange since at some point, the outlet of the cold stream will be hotter than the outlet of the cold stream, resulting in a reverse heat exchange.

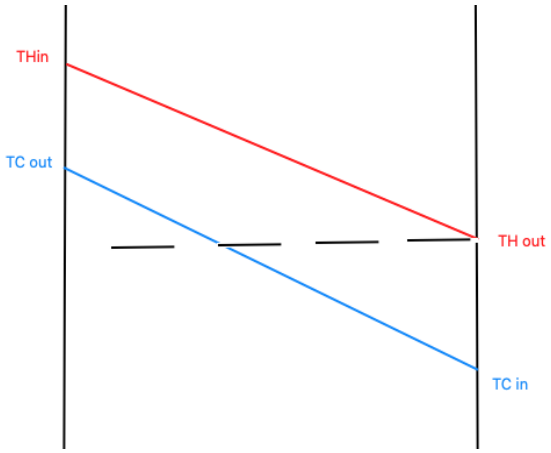

Figure 22: Temperature crossing

To eliminate this issue, counter-current flow heat exchangers can be used, where the outlet temperature of the hot side can be lower than the outlet temperature of the cold stream. Counter current heat exchangers can have a temperature cross because the temperature cross will occur at different points between the outlets, with the usage of multiple tubes and fins. Counter current flow heat exchangers are possible to perform heat exchange between steam and air. A counter-current heat exchanger where temperature cross is possible is the U-shaped counter-current heat exchanger, where due to the U-shape there is a greater heat exchange area (68).

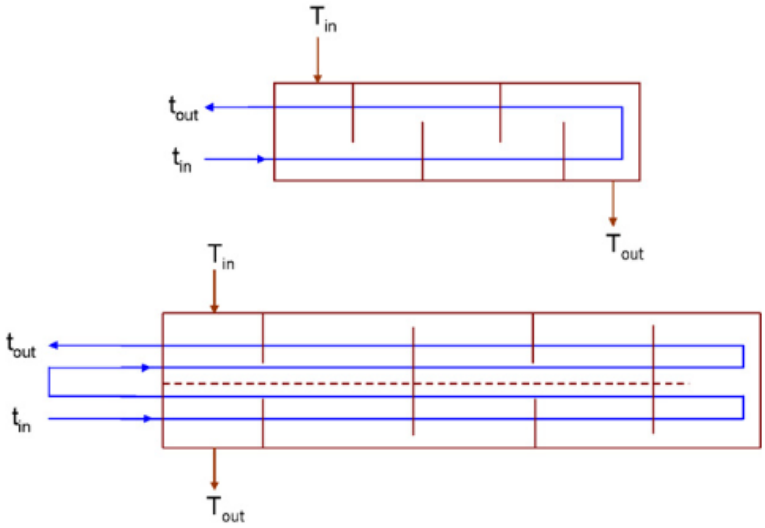

***Figure 23:Counter current heat exchanger. Licensed** from Elsevier (68)*

For heat exchangers, while calculating the operating temperatures, it is important to calculate the Logarithmic Mean Temperature Difference (LMTD), which shows the temperature driving force. The larger the LMTD the more the heat that is going to be exchanged, while if it is negative, it means that the heat transfer cannot take place. LMTD is affected by the cold stream inlet temperature, cold stream outlet temperature, hot stream inlet temperature, and hot stream outlet temperature.

$$LMTD = \frac{(Thot\ in - Tcold\ out) - (Thot\ out - Tcold\ in)}{ln\frac{(Thot\ in - Tcold\ out)}{(Thot\ out - Tcold\ in)}}$$

3.4 Concentrated solar thermal collectors

At the concentrated solar thermal collectors, there will be direct production of saturated steam, which is a novel solution. The outlet is saturated steam, containing the latent heat acquired from the sun's radiance, that goes in the heat exchanger to heat the air. In the case it would become superheated due to increased temperature or insufficient pressure, a desuperheater would be needed and it would increase the cost.

In order to produce the calculated steam, concentrated solar thermal collectors from Absolicon are going to be deployed. Based on the mass flow, simulations will take place using the software DLR Greenius which offers the option to simulate for several solar heat applications. The application chosen is concentrated solar thermal collectors for process heat. This state-of-the-art concentrated solar thermal collector has a maximum optical efficiency of 76.4 %.

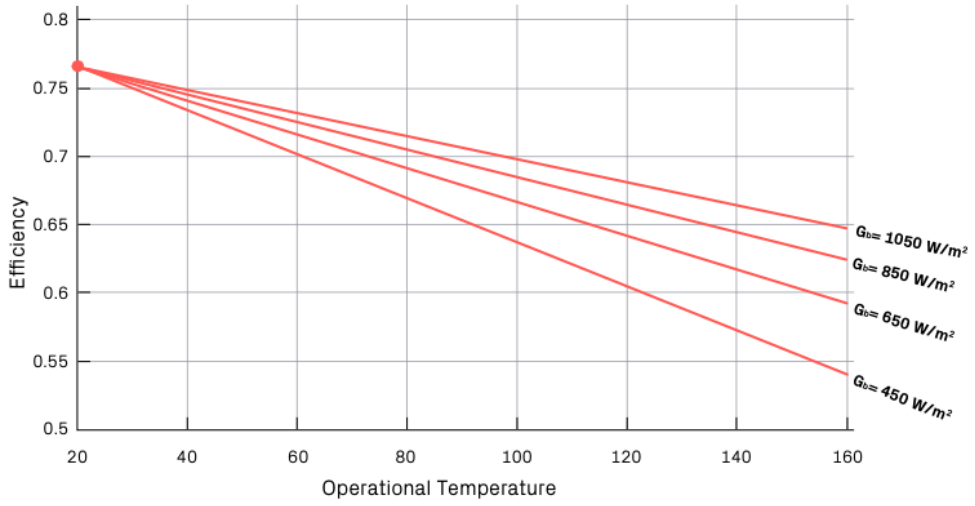

Figure 24: Absolicon's concentrated solar thermal collectors' efficiency as a function of solar radiation and operational temperature.

The parabolic trough chosen is an ordinary size for industrial concentrated solar thermal collectors, with a length of 5.1 meters and a width of 1 meter. The focal length chosen is 0.33 meters.

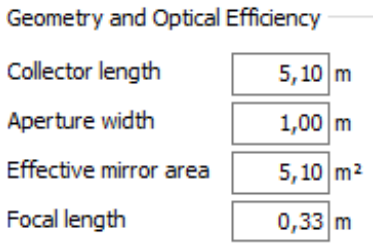

Figure 25: Parabolic trough collector dimensions at DLR Greenius

It is also important to set the distance between the rows and among the collectors when they are side by side. The distance between the rows stops the effect of shading from one row to the other while allowing space for the collector to move when tracking the sun. It also affects the size of the piping from one row to the other, as does the distance between the collectors, since the longer the piping between them, the more the heat losses induced.

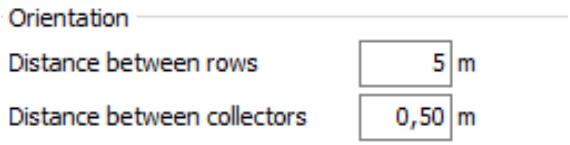

Figure 26: Distance between the collectors from DLR Greenius

The inlet temperature at the concentrated solar thermal collectors is calculated at 65 °C to be pressurized water. The desired output temperature is set to 170 °C of steam, which is the upper limit but possible output for the specific parabolic trough.

In this application, the concentrated solar thermal collectors have steam in the outlet and the following equation will be applied, considering the enthalpy of evaporation, to find the thermal power needed:

$$m = \frac{P \cdot 3600}{hfg} \qquad \text{(Eq.2)}$$

where:

m=mass flow of steam in kg/h
P=Power by steam in kW
h_{fg}= specific enthalpy of evaporation of steam at working pressure in kJ/kg

Absolicon's tool will also be utilized to calculate the area needed for this output. This simulator does not take into account the starting temperature of the heated fluid at the field. Also, the maximum temperature output possible for the calculations is 160 °C. DLR software on the other hand takes into account the starting and outlet temperature, the option if the output is pressurized water or steam as well as if it is a mix of water and glycol.

3.5 CO_2 emissions savings

Implementing environmentally sustainable solutions like solar heat to an application has an important impact on the environment. Many industries nowadays utilize natural gas or even oil in order to acquire thermal energy and steam. Modern natural gas boilers can achieve an efficiency of 90% but in this case, an existing 10- to 15-year-old boiler is considered, with 85 % efficiency. The efficiency of a boiler is the ratio of the total absorption heating value of outlet steam to the total supplied heating value. For every MWh of natural gas consumed, 204.8 kg of CO_2 are produced (69). To do this calculation, the total amount of natural gas consumed currently in the process is considered, since this is the amount of fossil fuel that will not be used. The calculations are done for 25 years, which is the expected lifespan of the collectors.

3.6 Net Present Value analysis

In order to find how feasible is the deployment of concentrating solar heat collectors, a Net Present Value (NPV) analysis has taken place to find the actual cost of the collectors in the expected 25-year lifespan. The calculations are done for 27 years since the first 2 years account for the licensing and construction when the field is not making any income. The cost of the collectors has been provided by Absolicon. Since the cost is heavily impacted by the solar field size and DLR software gave out a different field size than Absolicon's online simulator, two NVP analyses will take place, investigating if it is feasible in both cases. The following values will be calculated.

Capital Expenditure (CAPEX): Funds used by a company to acquire physical assets and in this case, the solar field.

Operational Expenditure (OPEX): Funds used by a company to keep the physical assets running. Equals 5% of the CAPEX in this case.

Discount rate: Function of the economy and company where the money is lent from. The most important economic parameter. For Greece, the rate is 3.75% in May 2023 (70).

Cash Flow: Amount of money that is saved from the solar field per year. It is calculated from the equation:

$$Cash\ flow = Gas\ price\ in \frac{€}{MWh} \cdot Production\ per\ year\ in\ MWh$$

Discounted Cash Flow: Value of money changing due to inflation. This comes from the equation:

$$Discounted\ cash\ flows = \frac{Cash\ flow\ of\ the\ year}{(1+Discount\ rate)^{year}}$$

NPV shows if the project is profitable after the specified period. If it is positive, it means that is likely to be profitable, if the is negative that it is not likely to be profitable and if it is zero, it means that it might be either profitable or costly. It is calculated as:

$$NPV = Discounted\ Cash\ Flows - CAPEX - SUM\ of\ discounted\ OPEX. \quad \text{(Eq 6.)}$$

Year 0: Decision moment: to decide whether to move forward with the investment or not.
Year 1&2: Permits, project, and construction work time.

Since the pricing of the collectors is based on many variables, like the price of mirrors, glass, and metals in the future the price may change. Similarly, the price of natural gas may change and affect the feasibility of the implementation of the solar field. Therefore, there will be four cases per simulation result. The first is with the cost of collectors at 400 €/m^2 and the natural gas cost stays constant, the second with 350 €/m^2 and the natural gas cost stays constant, the third if the cost of collectors stays at 400 €/m^2 but the gas price increases to 150 € and the fourth one if the price of the collectors decreases at 350 €/m^2 but the gas price increases to 150 €.

According to current macroeconomics, the investment has a CAPEX of 400 €/m^2 and this is the most likely scenario to happen. Slightly less probable to happen is a reduction in the CAPEX down to 350 €/m^2. The cost of the gas is important since it will lead to save money that can be directly used in this project. There is a most likely scenario which considers that the gas price stays constant. However, it is not unlikely that a higher price might occur, thus a scenario of 150 €/MWh was also included in the weighted NPV calculation.

4. Results

4.1 Process description

The spray drying process needs steam in order to heat the air that is going to dry the food. This steam will come from concentrated solar thermal collectors that can be installed in the facility, either on the roof or on the ground in a solar field, which is available, providing steam at 170°C and 8 $x10^6$ Pa in order to have saturated steam for better heat exchange. The proposed process will be comprised of the following steps:

1. A regeneration air cooler is used where the incoming water temperature is at 28 °C. Then it will be preheated from the hot mix exiting from the spray dryer to 58 °C. This step is deployed to utilize the waste heat from the hot stream of the exit of the spray dryer to preheat the water, to save energy instead of heating it from 28 °C to 170 °C with the concentrated solar thermal collectors.

2. A pump will increase the pressure to 8 $x10^6$ Pa.

3. The concentrated solar thermal collectors will use the solar heat and heat the water to 170 °C, at 8 $x10^6$ Pa to become saturated steam. The saturated steam will exchange the latent heat, and some sensible heat, with the air. Superheated steam would require de-superheating with the spraying of water or other methods to facilitate heat exchange.

4. The produced heating mean will go through the heat exchanger to heat the dry air to 160 °C, which is required for the spray drying. The air comes slightly preheated at 45 °C, since the ambient temperature, being an industry, is over 25 °C. The exit of the steam, being a condensate, will go to another process, the milk pasteurization. This is an energy-demanding processes where milk is heated up to 70 °C, as discussed with the engineers in place, and the waste stream can offer this. Then, it comes back as supply water at step 1.

5. The hot dry air is then led to the spray dryer to be sprayed on the food, to dry it, and then it exits from the dryer at 80 °C. At this stage it is the dried air that entered as well as the humidity captured from the food, going to the regen air cooler the heat up the supply water.

The process is displayed in the following figure, which has been done in cooperation with the food industry described. The two heat exchangers could be bought from the factory.

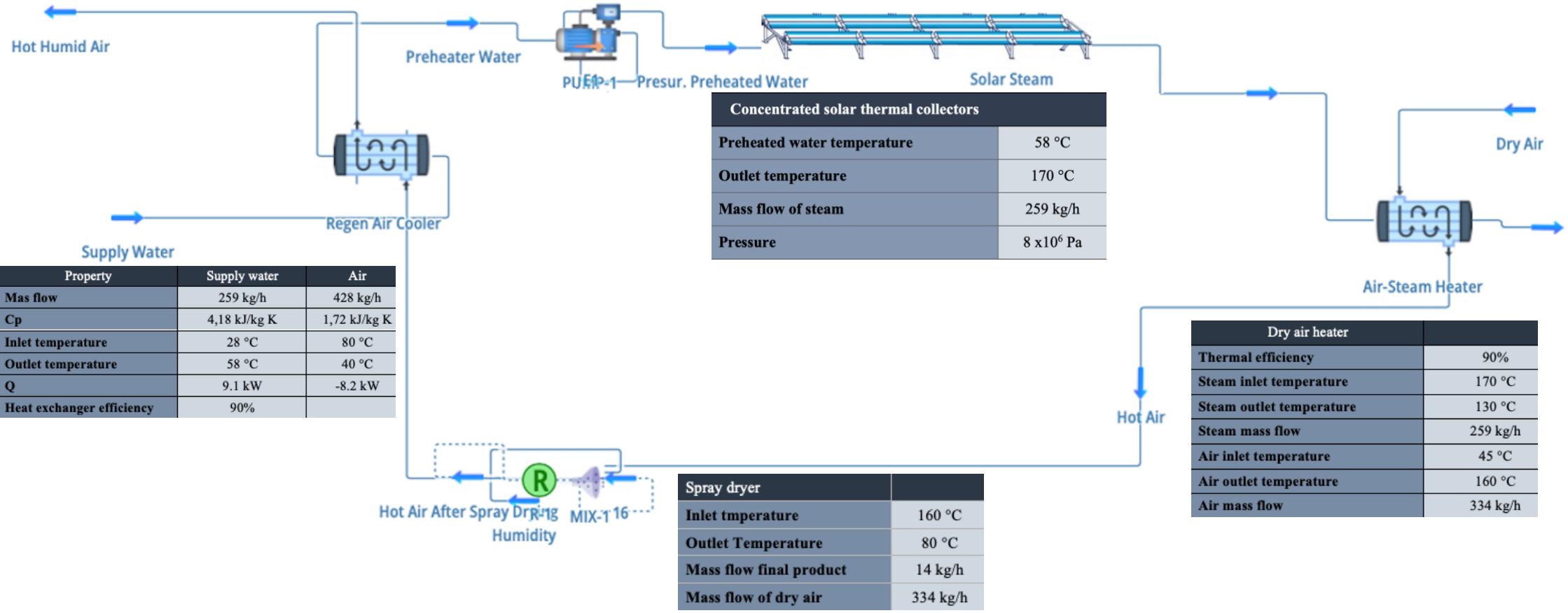

Concentrated solar thermal collectors	
Preheated water temperature	58 °C
Outlet temperature	170 °C
Mass flow of steam	259 kg/h
Pressure	8 x10^6 Pa

Property	Supply water	Air
Mas flow	259 kg/h	428 kg/h
Cp	4,18 kJ/kg K	1,72 kJ/kg K
Inlet temperature	28 °C	80 °C
Outlet temperature	58 °C	40 °C
Q	9.1 kW	-8.2 kW
Heat exchanger efficiency	90%	

Dry air heater	
Thermal efficiency	90%
Steam inlet temperature	170 °C
Steam outlet temperature	130 °C
Steam mass flow	259 kg/h
Air inlet temperature	45 °C
Air outlet temperature	160 °C
Air mass flow	334 kg/h

Spray dryer	
Inlet tmperature	160 °C
Outlet Temperature	80 °C
Mass flow final product	14 kg/h
Mass flow of dry air	334 kg/h

Figure 27: Spray drying process per kg/h of steam consumed

4.2 Process calculations

4.2.1 Drying conditions

It was found out that at 160 °C inlet temperature of the air to the spray dryer, the density is 0.814 kg/m^3 (65). The tested inlet volume flow was 411 m^3/h, in order to have a continuous reference as above. Thus, the mass flow of air is:

$$0.814\ \frac{\text{kg}}{\text{m3}} \cdot 411\ \frac{\text{m3}}{\text{h}} = 334.6\ \frac{\text{kg}}{\text{h}} \text{of air}$$

Based on Schmitz-Schug et.al pilot scale tests, the selected water contect of 4 % to 6 % corresponds to 14 kg/h of product mass flow rate. Similarly, the outlet temperature corresponds to 80 °C (65). To further support these calculations, Koca *et al*. have found out that an inlet temperature of 160 °C corresponds to 80 °C outlet temperature and a pressure of 4.4 x10^6 Pa (71). The following table sums up the conditions at this stage.

Table 2: Spray dryer properties

Spray dryer	
Inlet tmperature	160 °C
Outlet Temperature	80 °C
Mass flow final product	14 kg/h
Mass flow of dry air	334 kg/h

4.2.2 Dry-air heat exchanger

At this stage, there are 334 kg/h of hot dry air going to the spray dryer at a temperature of 160 °C to dry the food instantaneously. This dry air has passed through a steam-air heat exchanger to be heated. The air comes in at 45 °C and exits at 160 °C.

Assuming an efficiency of the steam-to-air heat exchanger of 90 %, thus 90 % of the energy coming from the produced steam is transferred to heat for the air (72). The following results occur and thus the required steam mass flow is:

Table 3: Heat exchanger properties

Property	Steam	Dry Air
Mass flow	259 kg/h	334 kg/h
Cp	4.2 kJ/kg K	1.02 kJ/kg K
Inlet temperature	170 °C	45 °C
Outlet temperature	130 °C	160 °C
Q	-12.09 kW	10.88 kW
Heat exchanger efficiency	90%	

Thus, there is a steam flow of 259 kg/h incoming to the heat exchanger at a temperature of 170°C which heats up air from 45 °C to 160 °C. Then the condensate exits at 130 °C which then goes to heat up milk in the pasteurization process. In the meantime, the 160 °C outlet temperature of the air is required as discussed.

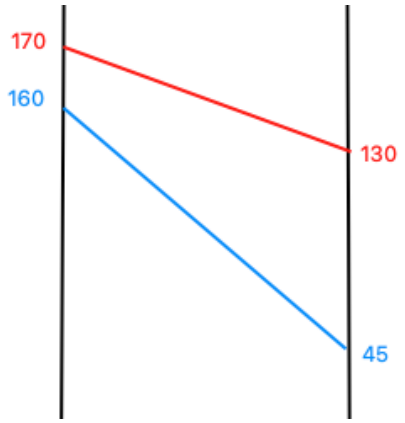

Figure 28: Steam air heat exchanger temperature range

Therefore, not all of the thermal energy of the collectors can be converted completely to heated air, because the temperature cross will be very high and will affect the heat exchange. If the collectors could reach a higher temperature, this would affect the rest of the heat exchange. The following table displays the conditions at the heat exchanger.

Table 4: Conditions at the heat exchanger

Dry air heater	
Thermal efficiency	90%
Steam inlet temperature	170 °C
Steam outlet temperature	130 °C
Steam mass flow	259 kg/h
Air inlet temperature	45 °C
Air outlet temperature	160 °C
Air mass flow	334 kg/h

4.2.3 Concentrated solar thermal collectors' conditions

The output of the collectors will be 259 kg/h of steam at 170 °C, when maximum radiation (1000 W/m^2) reaches the collector. Correlating the consumption to product yield, the result is that 259 kg/h of steam are converted to heated air to dry a food and the output is 14 kg/h of powder. The conditions at the concentrated solar thermal collectors are:

Table 5: Conditions at the concentrated solar thermal collectors

Concentrated solar thermal collectors	
Preheated water temperature	58 °C
Outlet temperature	170 °C
Mass flow of steam	259 kg/h
Pressure	8 x10^6 Pa

4.2.5 Supply water and waste heat stream heat exchanger preheat

The stage between the concentrated solar thermal collectors and the outlet of the spray dryer involves a step where the waste heat coming from the spray dryer, preheats the incoming supply water. This supply water receives heat from the exit of the spray dryer and is then arriving to the concentrating solar collectors. At the exit of the spray drier there is the dried air that entered, and also the humidity taken out of the food. Based on the initial reference for the spray dryer, the output during those conditions is 14 kg/h. The milk's water content is 87 %, meaning that the 107.7 kg/h of milk are entering the spray dryer in order to acquire 14 kg/h of powder eventually. That means that the water removed from the food is 93.7 kg/h. The outlet of the spray dryer is mostly air and the water removed from the food. This affects the heat capacity of the mixture and it is adjusted in analogy with the percentage of air and water. The conditions at the regeneration heat exchanger are:

Table 6: Conditions at regenerating heat exchanger

Property	Supply water	Air
Mas flow	259 kg/h	428 kg/h
Cp	4.18 kJ/kg K	1.72 kJ/kg K
Inlet temperature	28 °C	80 °C
Outlet temperature	58 °C	40 °C
Q	9.1 kW	-8.2 kW
Heat exchanger efficiency	90%	

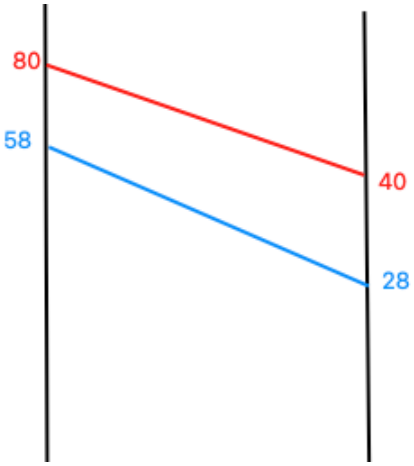

Figure 29: Spray dryer waste stream and supply water heat exchanger

In order to compare the steam consumption to product yield with the current installation, which is the drum drying, some data from the industry were taken. This is an upscale recommendation to achieve the same output. The aimed product yield is 150 kg/h in the industry chosen, not operating continuously but on variable shifts. In order to achieve this with the spray drying process, 2776 kg/h of steam will be required from the concentrating solar heat collectors to eventually receive 150 kg/h of dried product.

Table 7: Steam needs and dried food yield in kg/h

Property	
Steam needs	2776 kg/h
Dried food yield	150 kg/h

4.3 Comparison of steam consumption of current and proposed technology

It has been established that 2776 kg/h of steam are required to spray dry food and receive 150 kg/h of final product. With the currently installed drum drying technology, 3200 kg/h of steam are required to produce the same amount of dried food.

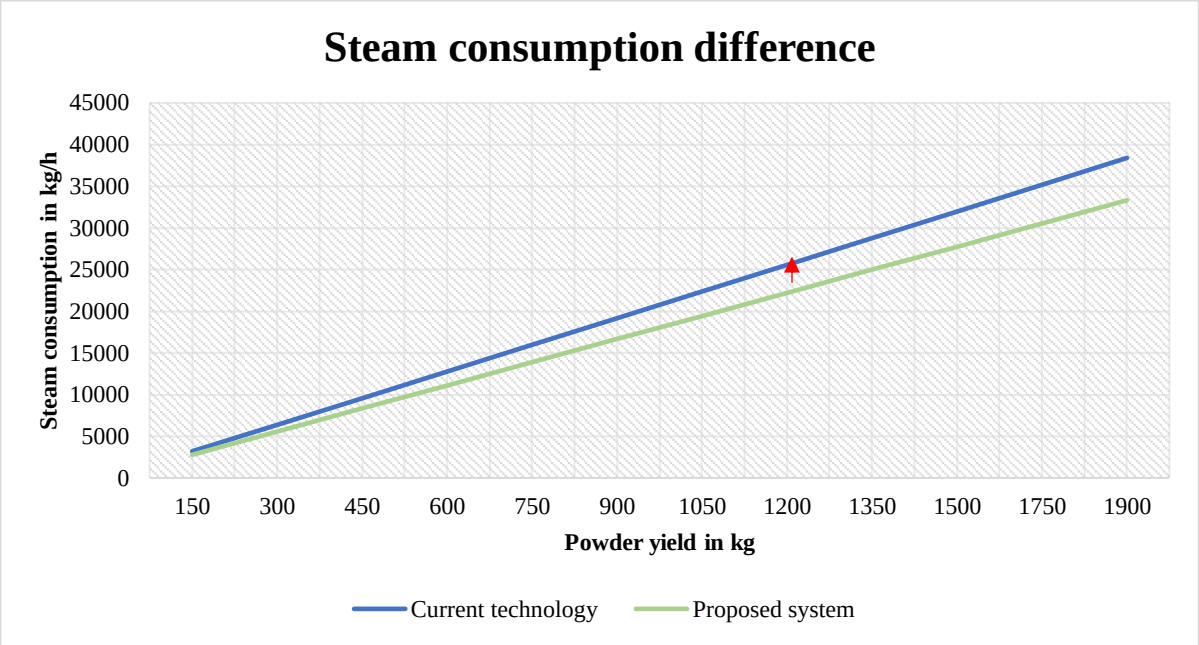

Figure 30: Current vs proposed system steam consumption

As it can be observed from the graph, because the annual production in the industry is not standard, the decrease in one hour of production is 424 kg of steam and in an 8-hour shift, it is 3392 kg of steam. This corresponds to 13.25 % decrease in steam needs. In the meantime, with the proposed system, there will also be heat given to the pasteurization process.

4.4 Simulations for concentrated solar thermal collectors

4.4.1 Greenius DLR

DLR Greenius software, like other simulation programs about solar, has the ability to simulate and give as an output the monthly and annual energy output in MWh. In the case of the upscaled system, an input of 2776 kg/h of steam is considered to be consumed by using the spray dryer to receive 150 kg/h of powder.

By converting the steam mass flow to thermal power, the result is 2134 kW based on Eq 2. According to Absolicon's online simulator, this corresponds to 2220 MWh per year. Absolicon's online simulator is a fast and easy tool to calculate the output of concentrating solar heat collectors. It is not possible to insert the exact power number, but to get an estimate. It also comes to show that the calculation above from steam mass flow to power was correct, since here 2.74 tons of steam/h correspond to 2130 kW, which is very close to the calculated

value. The simulations in DLR give the energy in MWh per year as an output, so this step is important to proceed.

Power	Energy
2130 kW	**2220** MWh/year
2.74 tons steam/h	**0.58** MWh/(year m²)

Figure 31: Results from Absolicon's online simulator

The simulations start with the setting of the location and the acquisition of the weather file, which averages the incoming radiation throughout 15 years. In order to achieve the required steam thermal energy, many simulations have taken place and the results are displayed below.

Field parameters

	Field/Superheater
Number of rows in the field	23
No. of collectors/row (loop)	18
Field size (effective mirror area)	2111 m²

Figure 32: Concentrated solar thermal collectors' size based on DLR calculations from DLR Greenius

Typical Operation Year

The thermal output of the collector field is 2229,85 MWh/a.
The specific thermal output is 1056 kWh/m² collector area.
The anual solar share (gross) is 100,0 %.

Figure 33: Annual thermal output of the collectors' field from DLR Greenius

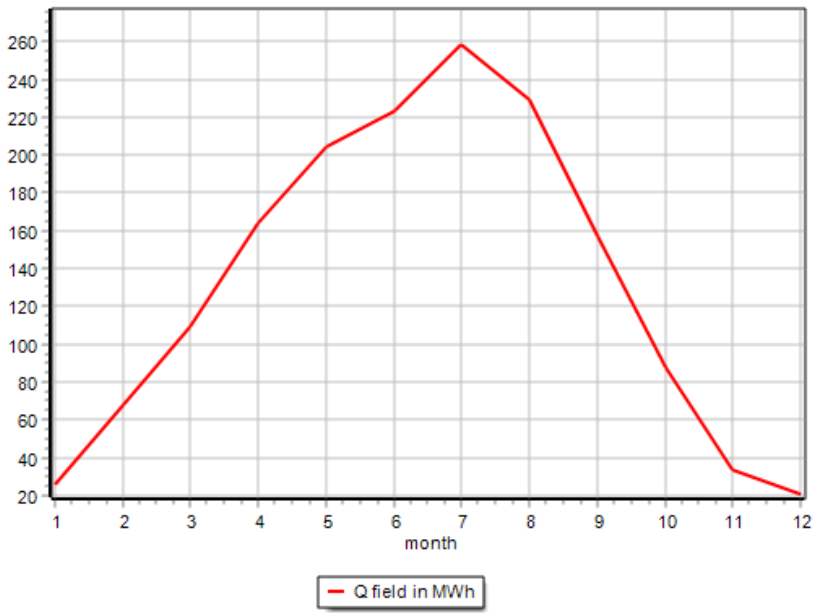

Figure 34: Monthly thermal energy output from DLR Greenius

In order to cover the annual process' needs, 2220 MWh of thermal energy is required. To achieve so, with the chosen concentrating solar collector and by using the DLR software, 23 rows with 18 collectors per row are required, resulting in 2111 m^2 of effective mirror area. As it can be seen in the figure below, the collectors are placed as close as possible to the industry to minimize heat losses and cost from the piping.

Figure 35: Solar field size in the installation

4.4.2 Absolicon's online simulator

Absolicon's online simulator has calculated that for the same output, 3833 m^2 of collectors are required.

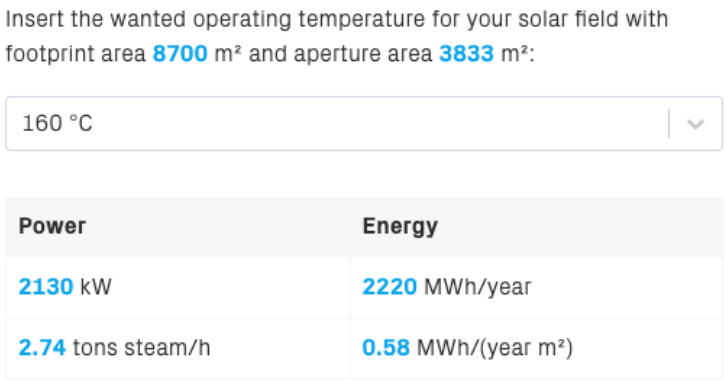

Figure 36: Field size with Absolicon's online simulator

Due to the difference in the required solar field between the DLR Greenius simulator and Absolicon's online simulator, calculations took place to understand and explain the difference, based on the solar radiance in Athens, Greece which is close to Agrinio, Greece. The reason for the different cities is that Athens is the capital, and more weather data is available. The following graph shows the radiation per month per hour in Athens, on average for the last 25 years. It can be seen that for 8 hours per day, there is radiation for powering the collectors.

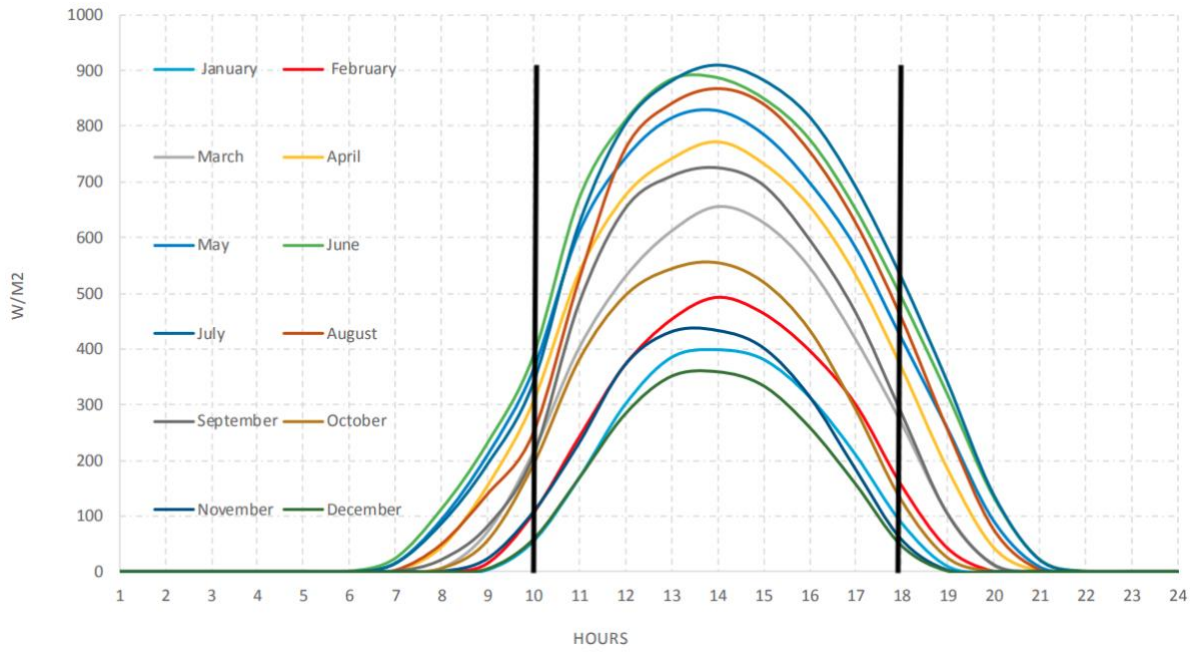

Figure 37: Radiation in Athens during the last 25 years (73)

Based on the radiation from the graph, the total radiation per year can be calculated taking into account two scenarios, one with 8-hour shifts only on weekdays and one with 8-hour shifts including also weekends. These calculations are to determine which simulation software is closer to which scenario. They are not as accurate as the two simulators, since the radiation is in average but based on scientific data.

Table 6: Two scenarios regarding the weekend shifts and the useful annual output

	Weekdays shift	Whole wheek shifts	Units
May to August	4	4	months
Average radiation	800	800	W/m^2
Operating days per month	22	30	days
Operating hours per month	704	960	hours
Output	563	768	kWh/m^2
April-March-September-October	4	4	months
Average radiation	550	550	W/m^2
Operating days per month	22	30	days
Operating hours per month	704	960	hours
Output	387	528	kWh/m^2
November to February	4	4	months
Average radiation	300	300	W/m^2
Operating days per month	22	30	days
Operating hours per month	704	960	hours
Output	211	288	kWh/m^2
Annual output	1162	1584	kWh/m^2
Total hours	2112	2880	hours

Therefore, based on whether there are shifts during the weekend or not, the total radiation received output is calculated during the industry's operation. The following table shows calculations based on the radiation of Figure 37.

Table 7: Output based on the weekend shifts and comparison with simulation methods

	Weekdays shifts	Whole week shifts	Units
Average efficiency	60	60	%
Average radiance	500	500	W/m^2
Average power output per collector	1.5	1.5	kW per collector
Average energy output per collector	1.53	1.53	kWh per collector
Total hours calculated	2112	2880	hours
Energy output per collector per year	3.23	4.4	MWh per year
Energy requirement	2220	2220	MWh per year
Number of collectors	687	504	collectors
Area of collector	5.1	5.1	m
Area required	**3504**	**2569**	m^2
Area calculated with DLR Greenius	2111	**2111**	m^2
Area calculated with Absolcion's simulator	**3833**	3833	m^2

Thus, the area required is close to Absolicon's calculation if the industry operates with 8-hour shifts during weekdays, while it is closer to DLR Greenius calculations when it operates with 8-hour shifts during weekdays and weekends as well.

4.5 CO_2 emissions saved

It has been calculated that 2220 MWh are required per year to operate the spray dryer, which in this case are suggested to be provided by solar heat to minimize the use of fossil fuels. To calculate the emissions saved, similar to the case of converting the steam mass flow of the collectors to energy, 3200 kg/h of steam correspond to 2526 MWh per year. This is the amount of steam that would be used in the case of the existing technology and natural gas as a fuel.

Table 8: CO_2 reduction in 25 years

Property	Quantity	Unit
Required energy	2526	MWh
Used from natural Gas boiler	2972	MWh
CO_2 per MWh	204.8	kg/MWh
Yearly CO_2 reduction	609	tn of CO_2
CO_2 reduction in 25 years	15215	tn of CO_2

In order to show the impact of the suggested system on the environment, the average mass of CO_2 absorbance per year is 21kg (74). The following table shows that the equivalent trees required to be planted in order to absorb this amount of CO_2, are 28982.

Table 9: Equivalent trees planted to compensate for the CO_2 reduction in 25 years

Property	Quantity	Unit
CO_2 absorbed from a tree per year	21	kg
CO_2 absorbed from a tree in 25 years	0.525	tons
Number of trees planted to absorb this CO_2	28982	trees

4.6 Net Present Value analysis

4.6.1 NPV using DLR software

It has been found out that DLR software has calculated that 2111 m^2 of collectors are required to have an output of 2220 MWh annually. The following table represents the scenario where the cost of the collectors is 400 €/m^2. Is it shown as a reference, since the rest of the three scenarios will be presented as a summary.

Table 9a Economic properties for case 1

Solar Field (CAPEX)	400	€/m^2
OPEX	5%	•CAPEX
Area	2111	m^2
Discount rate	3.75%	
Gas price	120	€/MWh
Production per year	2220	MWh

Initial Investment (CAPEX)	**844,400**	€

Table 9b Economics for case 1 for 27 years

Year	SUM	1&2	3	4	5	6	7	8	9
Cash Flows €			266400	266400	266400	266400	266400	266400	266400
Discounted Cash Flows €	3970536		238545	229923	221612	213602	205882	198440	191268
OPEX before discount rate €	1055500		42220	42220	42220	42220	42220	42220	42220
OPEX after discount rate €	629264		37805	36439	35122	33852	32629	31449	30313

Year	10	11	12	13	14	15	16	17	18
Cash Flows €	266400	266400	266400	266400	266400	266400	266400	266400	266400
Discounted Cash Flows €	184354	177691	171268	165078	159111	153360	147817	142474	137325
OPEX before discount rate €	42220	42220	42220	42220	42220	42220	42220	42220	42220
OPEX after discount rate €	29217	28161	27143	26162	25216	24305	23427	22580	21764

Year	19	20	21	22	23	24	25	26	27
Cash Flows €	266400	266400	266400	266400	266400	266400	266400	266400	266400
Discounted Cash Flows €	132361	127577	122966	118521	114237	110108	106128	102292	98595
OPEX before discount rate €	42220	42220	42220	42220	42220	42220	42220	42220	42220
OPEX after discount rate €	20977	20219	19488	18784	18105	17450	16820	16212	15626

Table 9c NPV and cost reduction per MWH for case 1 after 27 years

NPV	**2,496,871**	**€**
Cost reduction per MWh	**45**	**€/MWh**

As it can been observed from the calculations, an initial investment of 844,400 € will have an NPV of 2,496,871 € in 27 years, meaning there will be a high profit. The cost per MWh can be reduced by 45 €/MWh from 120 €/MWh that it is now and stay constant.

The following sensitivity analysis takes in consideration different economic scenarios.

Table 10: Sensitivity NPV analysis of the 4 cases with DLR Greenius simulations

Case	NPV		Probability
400€/m^2 of collector and 120€/MWh of natural gas	2,496,871	€	30%
350€/ m^2 of collector and 120€/MWh of natural gas	2,681,079	€	20%
350€/ m^2 of collector and 150€/MWh of natural gas	3,673,713	€	20%
400€/ m^2 of collector and 150€/MWh of natural gas	3,489,505	€	30%
Weighted NPV	**3,066,872**	**€**	

It is observed that all four cases the NPV is positive and the average NPV is 3,066,872€, bringing a significant profit to the investor.

4.6.2 NPV using Absolicon's online simulator

Using Absolicon's online simulator, it was found out that 3833 m^2 of effective mirror area are required to have an annual output of 2220 MWh.

Table 11a Economic properties for case 1

Solar Field (CAPEX)	400	€/m^2
OPEX	5%	•CAPEX
Area	3833	m^2
Discount rate	3.75%	
Gas price	120	€/MWh
Production per year	2220	MWh
Initial Investment (CAPEX)	**1,533,200**	€

Table 11b Economics for case 1 for 27 years

Year	SUM	1&2	3	4	5	6	7	8	9
Cash Flows €			266400	266400	266400	266400	266400	266400	266400
Discounted Cash Flows €	3970536		238545	229923	221612	213602	205882	198440	191268
OPEX before discount rate €	1916500		76660	76660	76660	76660	76660	76660	76660
OPEX after discount rate €	1142572		68644	66163	63772	61467	59245	57104	55040

Year	10	11	12	13	14	15	16	17	18
Cash Flows €	266400	266400	266400	266400	266400	266400	266400	266400	266400
Discounted Cash Flows €	184354	177691	171268	165078	159111	153360	147817	142474	137325
OPEX before discount rate €	76660	76660	76660	76660	76660	76660	76660	76660	76660
OPEX after discount rate €	53050	51133	49285	47503	45786	44131	42536	40999	39517

Year	19	20	21	22	23	24	25	26	27
Cash Flows €	266400	266400	266400	266400	266400	266400	266400	266400	266400
Discounted Cash Flows €	132361	127577	122966	118521	114237	110108	106128	102292	98595
OPEX before discount rate €	76660	76660	76660	76660	76660	76660	76660	76660	76660
OPEX after discount rate €	38089	36712	35385	34106	32873	31685	30540	29436	28372

Table 11c NPV and cost reduction per MWH for case 1 after 27 years

NPV	**1,294,763**	**€**
Cost reduction per MWh	**23**	**€/MWh**

Absolicon's online simulator calculates that a larger area of collectors is required for the same output. In this case, the NPV is 1,294,763 € after 27 years and the cost reduction is 23 €/MWh. It is logical that is makes a lower profit that the DLR case because it calculates that the CAPEX and OPEX are higher for the same output.

Table 12: Sensitivity NPV analysis of the 4 cases with Absolicon's simulator

Case	NPV		Probability
400€/ m^2 of collector and 120€/MWh of natural gas	1,294,763	€	30%
350€/ m^2 of collector and 120€/MWh of natural gas	1,629,235	€	20%
350€/ $m^2$of collector and 150€/MWh of natural gas	2,621,869	€	20%
400€/ $m^2$of collector and 150€/MWh of natural gas	2,287,397	€	30%
Weighted NPV	**1,924,869**	**€**	

The average NPV with Absolicon's online simulator is 1,924,869 €, showing that in all four scenarios, there is a significant profit

5. Discussion

5.1 Research questions answers

The research questions which have come up for the writing of this thesis are therefore answered, based on the results of this thesis.

Research question 1: How can solar energy with direct steam generation be implemented in food industries in drying processes?

Solar energy is one of the most promising, used, and applicable renewable sources and can be well coupled with the food industry. The direct steam generation from concentrated solar thermal collectors can be used directly in processes or through heat exchangers in this case, providing thermal energy in various processes. Based on Figure 31 where the current and proposed system hourly steam consumption are compared, there is a decrease of 13.25 % leading to a decrease of 3392 kg of steam in an 8-hour shift in the industry.

As with any solar solution, the output from the concentrated solar thermal collectors from May to September and especially during summer is higher. Thus, the thermal energy acquired from the solar field will be higher during these months compared to winter months. Therefore, to fully exploit the energy captured by the sun, the shifts can be adjusted and increased during the summer months. In the case where the production was one 8-hour shift per time, there is a possibility to add shifts during the weekends.

Additionally, there were two calculation methods evaluated. DLR Greenius software considers the parameters of the collector as well as the inlet and outlet temperature of the collector. Absolicon's online simulator can reach a maximum of 160 °C and does not consider different inlet temperatures. The results showed that DLR Greenius calculates that 2111 m^2 are required while Absolicon's online simulator calculates that 3833 m^2 are required, for the output of 2220 MWh per year. After calculations based on average radiation of 25 years, it can be observed that DLR's calculations fit in the case of operating the industry with 8-hour shifts per day for every day of the week including the weekends, while Absolicon's online simulator fits closer to operating the industry with 8-hour shifts only during weekdays. Therefore, this gives the option to the industry to decide, based on the planned product yield and available personnel, the size of the solar field.

As far as it concerns production and scheduling, concentrating solar collectors' fields offer a device to measure the radiation, wind speed and temperature to adjust the performance. Based on this and previous weather data, a computer center could be used which by using machine learning and artificial intelligence, could predict the possible radiation and thus food production, making the user aware and scheduling the production and shifts. The existing steam network using natural gas or other fossil fuels can be kept in case additional production is required when the radiation is not sufficient. This makes the implementation of the solar field

logical to operate and give the required production throughout the year since powders offer a long shelf life and can be overproduced in the summer months and be sold throughout the year. The action of overproducing when the solar radiation is high and taking advantage of it, is a way of utilizing solar energy and having a yield from it. This could be a storage solution of solar power into food powder since otherwise it would not be utilized.

Furthermore, there is a significant difference in hourly steam consumption between the proposed system consisting of the spray dryer, the heat exchangers and the waste stream heat capture compared to drum drying. This difference comes to show the reduced consumption of the proposed technology and that eventually it is more sustainable. An important parameter is the heat transfer taking place since convection is transferring heat faster than conduction. On drum drying, there is steam on the inside of the drum transferring heat to the metallic drum through convection and then the metallic drum heats up through conduction the food on top of it. In the case of spray drying, the heat transfer is from steam to dry air through convection and then from the dried air to the food through convection as well. Therefore, spray drying by having only heat transfer though convection can be more efficient due to the faster heat transfer. The currently installed drum dryers initially could have a lower steam consumption but due to losses and mechanical deterioration over the years, the amount of steam requirements could have increased.

Research question 2: What is the environmental impact of using solar energy in an industry for spray drying?

During this thesis report, it has been shown that the implementation of an efficient solution like spray drying with solar thermal solutions, like concentrated solar thermal collectors, can offer a significant impact on the environment. In more detail, the deployment of a solar thermal pack has provided thermal energy for the spray drying process and the waste stream of this was guided to heat up milk in the pasteurization process. The outcome was a saving of 15,215 tones of CO_2 in the 25-year lifespan of the collectors. This corresponds to planting 28,982 trees to absorb this amount of CO_2 in 25 years. CO_2 is a greenhouse gas that is responsible for the worldwide average temperature increase. The implementation of this proposed system in the food industries worldwide could decrease CO_2 emissions vastly. Furthermore, in Table 1 calculations for CO_2 savings have taken place for the implementation of concentrated solar thermal collectors in various industries. The impact from the installation at the industries with an annual need in the same order of magnitude to the food one in discussion (brewery 1 and 3, manufacturing and district heating) is 54,025 tones of CO_2 in the 25-year lifespan of the solar field, instead of using oil.

Research question 3: Is the investment in solar fields economically feasible?

It has been concluded, even though the two different simulation methods showed different aperture areas required for the same output, that in the 25-year lifespan of the collectors and the 2 years of construction, it is economically feasible to implement solar thermal parks for spray drying in the food industry. It provides a lower cost per MWh and very importantly keeps

it constant regardless of the changes in pricing of fossil fuels, making the industry more stable towards changes. In the case of DLR the weighted NPV comes out 3 million € and in the case of Absolicon's calculations the weighted NPV comes out to 1.9 million €, proving to be economically feasible as well. The economic feasibility of implementing concentrated solar thermal collectors in the food industry increases the possibility of further installation worldwide, since investors find it profitable, and thus increasing the environmental impact. The industry has the option to choose the size of the solar park based on the number of shifts operating per week, but both cases are profitable.

Research question 4: Are there any complications and bottlenecks in this process and how could they be solved?

In order to verify the results, it is preferred to make real-life experiments with all the components. The heat exchangers proposed were possible to be acquired by the specific food industry, although the heat exchange efficiency could be lower or higher. The implementation of heat exchangers with higher efficiency, especially on steam-to-air heat exchangers which can reach very high efficiency, is very costly and a comparison between a very efficient heat exchanger and its cost would be beneficial. One complication is the cross temperature found in the heat exchangers which can only be solved with counter-current heat exchangers with multiple tubes, as suggested in this case. After performing experiments, it could be possible to try a lower product yield and lower the inlet air temperature, allowing a recirculation of the condensate of the steam after the heat exchanger, instead of going to the pasteurization process. Furthermore, an increased outlet temperature from the concentrating solar collectors could lead to a lower mass flow of steam and thus field size, making it more economically feasible.

5.2 Limitations

This report in the feasibility analysis does not take into consideration the acquisition of the spray dryer because it is a commercially available product, and the price depends on the manufacturer, the aimed annual yield, and the location of the industry. This cost could be compared with the cost of buying and installing a drum dryer, which requires the further building of a costly special clean room because the food produced is in direct contact with the environment and people operating it. During the feasibility study, the implementation of solar thermal parks using concentrated solar thermal collectors is assessed. Furthermore, in the emissions reduction calculations, the calculated result comes from not using fossil fuels to produce steam and does not include an LCOE analysis of the collectors building because it is not provided.

5.3 Suggestion for further research

The primary aspects of the process designed are the energy savings, the CO_2 emissions reduction and the feasibility of the investment. As far it concerns energy savings, those could be increased with an increased efficiency on the heat exchangers, resulting in better heat transfer and thus lower losses. This can reduce the steam requirements, the emissions, the solar

field size, and cost. Similarly, increased efficiency and outlet temperature of the concentrated solar thermal collectors can contribute to the same results. Furthermore, additional simulations for an exact amount of concentrated solar thermal collectors can take place to define the solar field size in more detail.

6. Conclusions

As a result of this investigation, a food drying system is proposed consisting of a spray dryer, an air-to-steam heat exchanger and a solar field with concentrated solar thermal collectors that is able to produce steam. The results show that less steam is required. This means that the industry with annual thermal energy needs of 2220 MWh for the spray drying process, can run entirely on solar thermal energy bringing therefore sustainability to the food industry. For this heat to be produced from solar, 2111 m^2 of collector aperture area are required, with solar concentrating collectors with a one-axis tracking system to be installed in a solar field close to the factory, in the case the industry operates with 8-hour shifts everyday including the weekends. In the case the industry operates only during weekdays with 8-hour shifts, the solar field size is 3833 m^2.

Economically wise, CAPEX and OPEX were estimated after discussions held with the equipment manufacturers and the factory operating company. On the base case scenario if the industry operates every day of the week including weekends, the NPV of such investment is 844,400 €. Three more cases have been evaluated with a probability occurrence for each case, giving a weighted NPV of 3 million € after 27 years, which is the expected 25 years lifespan of the collectors and the 2 years of construction. In the case the industry operates only on weekdays, the investment costs 1,533,200 € and the weighted NPV is 1.9 million €. This creates a possible sustainable pathway to decarbonize the food industry while keeping the energy costs low, resulting in lower costs for the industry and thus the consumer.

The proposed system has resulted in a 424 kg/h of steam reduction for the same product yield, which is a 13.25 % reduction compared with the existing technology. During this process, there are two waste heat recovery points to decrease the wasted heat and reduce the energy requirements, while another energy-consuming process is partially covered. Overall, the proposed system shows a higher efficiency compared to the existing one.

Furthermore, the proposed system showed a significant positive environmental impact. With the decreased steam consumption and the implementation of renewable sources, sustainability is promoted to achieve SGDs. The proposed system showed a decrease of 15,215 tons of CO_2 during the 25-year lifespan of the solar field, which is a significant reduction of scope 1 emissions.

Throughout simulations it was possible to calculate the heat produced and to calculate the price reduction per MWh of energy for natural gas in Greece. Moreover, using an abundant resource (solar energy) makes it an important step towards energy security and stable cost of operation of the process, since it is not dependent on the gas price fluctuations. This makes the process not only more sustainable, with zero emissions in the energy production, but with less economic risks.

This thesis shows a pathway on how the food drying process can decarbonize itself towards a sustainable and zero emission way, while assuring a lower heat cost, making milk powders more easily accessible to people around the world, due to decreased prices.

References

1. Our world in data. Environmental impacts of food production [Internet]. Available from: https://ourworldindata.org/environmental-impacts-of-food

2. Sustainable development goals [Internet]. Available from: https://sdgs.un.org/goals

3. Harvard business review. Global Demand for Food Is Rising. Can We Meet It? [Internet]. Available from: https://hbr.org/2016/04/global-demand-for-food-is-rising-can-we-meet-it

4. http://www.kerone.com/drum-dryers.php.

5. Doing machine drum dryer [Internet]. Available from: http://www.doingmachine.com/Rotary-Scraper-Drum-Dryer-pd41725086.html

6. Hammami, C., Rene, F., Determination of Freeze-Drying Process Variables for Strawberries, Journal of food Engineering, 1997.

7. Ullum, T.; Sloth, J.; Brask, A.; Wahlberg, M. Predicting spray dryer deposits by CFD and an empirical drying model. Drying Technology 2010.

8. Mansour, A.; Chigier, N. Air-blast atomization of non- Newtonian liquids. Journal of Non-Newtonian Fluid Mechanics 1995.

9. Kemp IC, Hartwig T, Herdman R, Hamilton P, Bisten A, Bermingham S. Spray drying with a two-fluid nozzle to produce fine particles: Atomization, scale-up, and modeling. Dry Technol. 2016 Jul 26;34(10):1243–52.

10. Kemp, I.C.; Oakley, D.E. Modelling of particulate drying in theory and practice. Drying Technology 2002.

11. Pinto, M.; Kemp, I.C.; Hartwig, T.; Bisten, A.; Bermingham, S. Development of an axisymmetric population balance model for spray drying and validation against experimental data and CFD simulations, 2014.

12. Cano-Chauca, M.; Stringheta, P.C.; Ramos, A.M.; Cal-Vidal, J. Effect of the carriers on the microstructure of mango powder obtained by spray drying and its functional characterization. Innovative Food Science and Emerging Technologies, 2005.

13. Bhandari, B.R.; Data, N.; Howes, T. Problems associated with spray drying of sugar-rich foods. Drying Technology 1997.

14. Ferrari CC, Germer SPM, De Aguirre JM. Effects of Spray-Drying Conditions on the Physicochemical Properties of Blackberry Powder. Dry Technol. 2012 Feb;30(2):154–63.

15. Quek, S.Y.; Chok, N.K.; Swedlund, P. The physicochemical proper- ties of spray-dried watermelon powder, 2007.

16. Rodr´ıguez-Herna´ ndez, G.R.; Gonza´ lez-Garc´ıa, R.; Grajales-Lagunes, A.; Ruiz-Cabrera, M.A.; Abud-Archila, M. Spray-drying of cactus pear juice (Opuntia streptacantha): Effect on the physicochemical properties of powder and reconstituted product, 2005.

17. Goula, A.M.; Adamopoulos, K.G. A new technique for spray drying orange juice concentrate. Innovative Food Science and Emerging Technologies 2010.

18. Obo´ n, J.M.; Castellar, M.R.; Alacid, M.; Ferna´ ndez-Lo´ pez, J.A. Pro- duction of a red–purple food colorant from Opuntia stricta fruits by spray drying and its application in food model systems. Journal of Food Engineering 2009.

19. Goula, A.M.; Adamopoulos, K.G. Spray drying of tomato pulp: Effect of feed concentration. Drying Technology 2004.

20. Kurozawa, L.E.; Morassi, A.G.; Vanzo, A.A.; Park, K.J.; Hubinger, M.D. Influence of spray drying conditions on physicochemical properties of chicken meat powder, 2009.

21. Isik S, Yildiz C. A new spray dryer supported with freely rotatable propellers enables more efficient drying of milk samples. Therm Sci. 2022;26(2 Part C):1871–82.

22. Islam MT, Shahir S, Uddin TI, Saifullah A. Current energy scenario and future prospect of renewable energy in Bangladesh.

23. RFF Recourses of the future. Global Energy Outlook 2023: Sowing the Seeds of an Energy Transition.

24. IEA. (2020) World energy balances.

25. S. H. Farjana, N. Huda, M. A. P. Mah- mud, and R. Saidur. Solar industrial process heating systems in operation - current ship plants and future prospects in Australia.

26. IED, 2010/75/EU.

27. Energy statistics - an overview. Available from: https://ec.europa.eu/eurostat/statistics-explained/index.php?title=Energy_statistics_-_an_overview#Final_energy_consumption

28. Europa statistics [Internet]. Available from: https://ec.europa.eu/eurostat/statistics-explained/index.php?title=File:Total_final_energy_consumption_by_industrial_sector,_EU,_2021_(PJ).png

29. Eurostat statistics. Available from: https://ec.europa.eu/eurostat/statistics-explained/index.php?title=File:Total_final_energy_consumption_by_industrial_sector,_EU,_2021_(PJ).png

30. S. H. Farjana, N. Huda, M. P. Mah- mud, and R. Saidur. Solar process heat in industrial systems - a global review.

31. S. K. Verma, N. K. Gupta, and D. Rak- shit. A comprehensive analysis on advances in application of solar collectors considering design, process and working fluid parameters for solar to thermal conversion.

32. GP-ESTELA-SolarPACES_Solar-Thermal-Electricity-Global-Outlook-2016_Executive-Summary.

33. Cirocco L R, Belusko M, Bruno F, et al. Cirocco L R, Belusko M, Bruno F, et al. Controlling stored energy in a concentrating solar thermal power plant to maximise revenue.

34. Wang F, Cheng Z, Tan J, et al. Progress in concentrated solar power technology with parabolic trough collector system: A comprehensive review[J]. Renewable & Sustainable Energy.

35. Manju S, Sagar N. Progressing towards the development of sustainable energy: A critical review on the current status, applications, developmental barriers and prospects of solar photovoltaic.

36. Statista CSP installations [Internet]. Available from: https://www.statista.com/statistics/494169/global-installed-concentrated-solar-power-csp-capacity-by-key-country/

37. © 2020 The World Bank, Source: Global Solar Atlas 2.0, Solar resource data: Solargis.

38. https://www.solarpaces.org/csp-technologies/csp-projects-around-the-world/ [Internet]. SolarPaces CSP locations.

39. M. Imtiaz Hussain, C. Ménézo, and J.-T. Kim,. "Advances in solar thermal harvesting technology based on surface solar absorption collectors: A review,."

40. M. P. Islam and T. Morimoto. Advances in low to medium temperature non-concentrating solar thermal technology.

41. C Stanciu et al. Analysis of a flat plate collector for hot water domestic use - a sensitivity study.

42. Evangelisti et al. - 2019 - Latest advances on solar thermal collectors A com.

43. D. Gao, G. Gao, J. Cao, S. Zhong, X. Ren, Y. N. Dabwan, M. Hu, D. Jiao, T. H. Kwan, and G. Pei. Experimental and numerical analysis of an efficiently optimized evacuated flat plate solar collector under medium temperature.

44. A. Veera Kumar, T. Arjunan, D. Seeni- vasan, R. Venkatramanan, and S. Vijayan. Thermal performance of an evacuated tube solar collector with inserted baffles for air heating applications.

45. Kalogirou - 2014 - Solar Energy Collectors.

46. C. Jiang, L. Yu, S. Yang, K. Li, J. Wang, P. D. Lund, and Y. Zhang. A review of the compound parabolic concentrator (cpc) with a tubular absorber.

47. Tanveer and Tezcanli Guyer - 2013 - Solar assisted photo degradation of wastewater by

48. SolarPACES. SolarPACES technology characterization solar dish systems. Available at http://www.solarpaces.org/images/pdfs/solar_dish.

49. Carrión-Chamba W, Murillo-Torres W, Montero-Izquierdo A. Una revisión de los últimos avances de los colectores solares térmicos aplicados en la industria. Ingenius [Internet].

2021 Dec 7 [cited 2023 Mar 15];(27). Available from: https://ingenius.ups.edu.ec/index.php/ingenius/article/view/27.2022.06

50. Bellos - 2023 - Progress in beam-down solar concentrating systems.

51. O. A. López-Núñez, J. A. Alfaro-Ayala, O. Jaramillo, J. Ramírez-Minguela, J. C. Castro, C. E. Damian-Ascencio, and S. Cano-Andrade. A numerical analysis of the energy and entropy generation rate in a linear fresnel reflector using com- putational fluid dynamics.

52. D. Sakthivadivel, K. Balaji, D. Dsilva Win- fred Rufuss, S. Iniyan, and L. Suganthi. Solar energy technologies: prin- ciples and applications.

53. El Gharbi N, Derbal H, Bouaichaoui S, Said N. A comparative study between parabolic trough collector and linear Fresnel reflector technologies.

54. M. Cagnoli a, D. Mazzei b, M. Procopio a, V. Russo b, L. Savoldi a, R. Zanino a. Analysis of the performance of linear Fresnel collectors: Encapsulated vs. evacuated tubes.

55. 11MW Solar Power Towers of Seville, Spain [Internet]. Available from: https://www.amusingplanet.com/2013/08/the-solar-power-towers-of-seville-spain.html

56. Absolicon webiste [Internet]. Available from: https://connect.absolicon.com/hubfs/infographics_AbsoliconSolarCollectors_220317.pdf?hsCtaTracking=c860775b-228a-4576-aaf1-4370cb66487c%7C68c1273f-d162-4ee1-b0ac-8e7b0d96a6f0

57. G. Barone, A. Buonomano, C. Forzano, and A. Palombo. Chapter 6 - solar thermal collectors.

58. Ravi K. K. and Reddy K. S., “Thermal analysis of solar parabolic trough with porous disc receiver,” Applied Energy, 86: 1804-1812 (2009).

59. Dagan E., Muller M., and Lippke F., “Direct steam generation in the parabolic trough collector”, Report of Plataform Solar de Almeria, Madrid, 1992.

60. Zarza E., Rojas M. E., Gonzlez L., Caballero J. and Rueda J., “INDITEP: The first pre-commercial DSG solar power plant,” Solar Energy, 80 (10): 1270-1276 (2006).

61. Krüger D., Krüger J., Pandian Y., Feldhoff J. F., Markus E., Eickhoff M., Hennecke K., Kanjanaburi solar thermal power plant with direct steam generation – layout. 16th Solar PACES Conference, Perpignan, France, pp. 21-24 (2010).

62. Shamimun Nisha, Ram Kumar Pal and K. Ravi Kumar. Direct steam generation in parabolic trough solar collector: Analytical modelling for prediction of flow pattern. 2019.

63. Eduardo Zarza a, , Loreto Valenzuela a, Javier Leo´ n , Klaus Hennecke , Markus Eck , H.-Dieter Weyers, Martin Eickhoff. Direct steam generation in parabolic troughs: Final results and conclusions of the DISS project.

64. https://www.idfa.org/definition.

65. Schmitz-Schug et al. - 2013 - Impact of the spray drying conditions and residence.

66. Robertus Wahyu N. Nugroho a, Marko Outinen b, Outi Toikkanen b, Antti Heino b, Daisuke Sawada a, Orlando J. Rojas. Effect of water activity on the functional, colloidal, physical, and microstructural properties of infant formula powder.

67. Cheng et al. - 2019 - Optimising water activity for storage of high lipi.

68. Vengateson - 2010 - Design of multiple shell and tube heat exchangers .

69. Natural gas emissions kg of CO2/MWh produced [Internet]. Available from: https://ourworldindata.org/grapher/carbon-dioxide-emissions-factor

70. Discounte and interest rate [Internet]. Available from: https://tradingeconomics.com/greece/interest-rate

71. Koca N, Erbay Z, Kaymak-Ertekin F. Effects of spray-drying conditions on the chemical, physical, and sensory properties of cheese powder. J Dairy Sci. 2015 May;98(5):2934–43.

72. Orović et al. - 2018 - Efficiency and Losses Analysis of Steam Air Heater.

73. Koudouris et al. - 2017 - Investigation on the stochastic nature of the solar.

74. USDA CO2 from a tree abrorbance [Internet]. Available from: https://www.usda.gov/media/blog/2015/03/17/power-one-tree-very-air-we-breathe